



A PRELIMINARY STUDY OF POROUS CERAMICS WITH LOW THERMAL CONDUCTIVITY FOR APPLICATION IN BUILDINGS



**BACHELOR OF MANUFACTURING ENGINEERING
TECHNOLOGY (PROCESS AND TECHNOLOGY) WITH
HONOURS**

2022



**Faculty of Mechanical and Manufacturing Engineering
Technology**

**A PRELIMINARY STUDY OF POROUS CERAMICS WITH LOW
THERMAL CONDUCTIVITY FOR APPLICATION IN BUILDINGS**



Najmi Abdul Fattah Bin Mohd Salleh

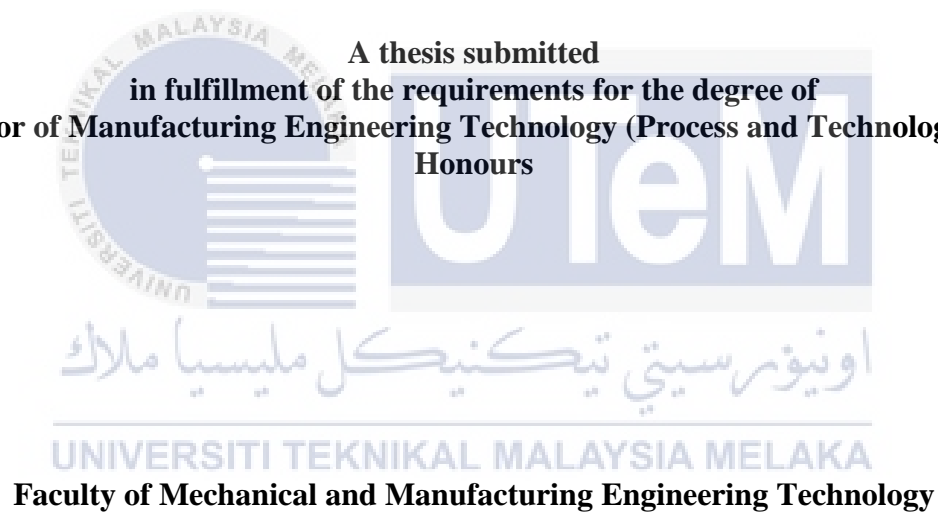
**Bachelor of Manufacturing Engineering Technology (Process And Technology) with
Honours**

2022

**A PRELIMINARY STUDY OF POROUS CERAMICS WITH LOW THERMAL
CONDUCTIVITY FOR APPLICATION IN BUILDINGS**

NAJMI ABDUL FATTAH BIN MOHD SALLEH

**A thesis submitted
in fulfillment of the requirements for the degree of
Bachelor of Manufacturing Engineering Technology (Process and Technology) with
Honours**



UNIVERSITI TEKNIKAL MALAYSIA MELAKA

2022

DECLARATION

I declare that this Choose an item. entitled “A Preliminary Study Of Porous Ceramics With Low Thermal Conductivity For Application In Buildings ” is the result of my own research except as cited in the references. The Choose an item. has not been accepted for any degree and is not concurrently submitted in candidature of any other degree.

Signature

:

Name

:

NAJMI ABDUL FATTAH BIN MOHD SALLEH

Date

:

18/01/2022

اونيورسيتي تيكنيكل مليسيا ملاك

UNIVERSITI TEKNIKAL MALAYSIA MELAKA

APPROVAL

I hereby declare that I have checked this thesis and in my opinion, this thesis is adequate in terms of scope and quality for the award of the Bachelor of Manufacturing Engineering Technology (Process and Technology) with Honours.

Signature :

Supervisor Name : *ASSOC. PROF. TS. DR. UMAR AL-AMANI BIN HAJI AZLAN*

Date :

18 / 1 / 2022

اونیورسیتی تکنیکل ملیسیا ملاک

UNIVERSITI TEKNIKAL MALAYSIA MELAKA

DEDICATION

In the name of Allah, the Most Merciful, and with heartfelt gratitude to the Prophet Muhammad S.A.W., I completed this job successfully and on time. Alhamdulillah, praise be to Allah for His mercy, I completed this project effectively and on time.

To express my heartfelt gratitude and heartfelt appreciation to my mother, Salwa binti Omar, and father, Mohd Salleh bin Abdul Rahman, for their support and sacrifice throughout this journey, both mentally and physically, I'd like to take this opportunity to express my heartfelt gratitude and heartfelt appreciation to them.

Hopefully, Allah will shower upon you all goodness and success in this life as well as the

next.

ABSTRACT

The microstructure of the tile surface, as well as the surrounding environmental and material factors, can all have an impact on a person's thermal perception of heat. Floor surfaces that are too warm in open outdoor environments may be considered uncomfortable. Thermal effusivity is a property of semi-infinite substances that determines the temperature at their interface as soon as they come into complete contact with one another. It is more pleasant to the touch ceramic tiles with a crusty surface, and these tiles can be used to reduce the temperature of a space by reflecting heat back into it. Included pores cause materials with poor conductivities and densities, which are the outcome of the inclusion of pores. The circumstances around the processing play a part in this. Although pores are not always indicative of a lack of mechanical strength, the existence of pores can be. Specifically, the purpose of this research is to evaluate the thermal and mechanical comfort of ceramic flooring manufactured from industrial atomized ceramic powder that incorporates refractory raw materials. Touch, according to theoretical and experimental examinations, enhances the porosity and crustiness of a surface, as well as the level of comfort it provides.



ABSTRAK

Struktur mikro permukaan jubin, serta faktor persekitaran dan bahan sekeliling, semuanya boleh memberi kesan kepada persepsi haba seseorang terhadap haba. Permukaan lantai yang terlalu panas dalam persekitaran luar terbuka mungkin dianggap tidak selesa. Efusi terma ialah sifat bahan separa tak terhingga yang menentukan suhu pada antara muka mereka sebaik sahaja ia bersentuhan sepenuhnya antara satu sama lain. Ia lebih menyenangkan untuk disentuh jubin seramik dengan permukaan berkerak, dan jubin ini boleh digunakan untuk mengurangkan suhu ruang dengan memantulkan semula haba ke dalamnya. Liang yang disertakan menyebabkan bahan dengan kekonduksian dan ketumpatan yang lemah, yang merupakan hasil daripada kemasukan liang. Keadaan sekitar pemprosesan memainkan peranan dalam hal ini. Walaupun liang tidak selalu menunjukkan kekurangan kekuatan mekanikal, kewujudan liang boleh jadi. Secara khusus, tujuan penyelidikan ini adalah untuk menilai keselesaan terma dan mekanikal lantai seramik yang dihasilkan daripada serbuk seramik pengatoman industri yang menggabungkan bahan mentah refraktori. Sentuhan, mengikut peperiksaan teori dan eksperimen, meningkatkan keliangan dan kerak permukaan, serta tahap keselesaan yang diberikannya.



ACKNOWLEDGEMENTS

Alhamdulillah, praise to God for His assistance and guidance in enabling me to complete this Bachelor Degree Project 1 work. I am indebted to my supervisor, ASSOC. Prof. TS. DR. Umar Al-Amani bin Azlan, for assisting me with the research and providing information. I am indebted to everyone who aided me and guided me through the Bachelor Degree Project's completion.

Additionally, I'd like to thank all of my friends, particularly my classmates, who have been extremely helpful and supportive in order to assist me in completing this project. They have provided me with numerous suggestions about how to better my project.

I am eternally grateful to my parents for their love and support throughout my life and in all of the activities I have participated in. Additionally, I wanted to express my gratitude to everyone who assisted me directly or indirectly in completing my Bachelor Degree Project. I am extremely appreciative of all your assistance.

UNIVERSITI TEKNIKAL MALAYSIA MELAKA



اونيورسيتي تيكنيكل مليسيا ملاك

UNIVERSITI TEKNIKAL MALAYSIA MELAKA

TABLE OF CONTENTS

	PAGE
DECLARATION	
APPROVAL	
DEDICATION	
ABSTRACT	i
ABSTRAK	ii
ACKNOWLEDGEMENTS	iii
TABLE OF CONTENTS	v
LIST OF TABLES	vii
LIST OF FIGURES	viii
LIST OF SYMBOLS AND ABBREVIATIONS	xi
LIST OF APPENDICES	xii
CHAPTER 1 INTRODUCTION	13
1.1 Research Background	13
1.2 Problem Statement	14
1.3 Research Objective	15
1.4 Scope of Research	16
1.5 Significant of Study	17
CHAPTER 2 LITERATURE REVIEW	18
2.1 Introduction	18
2.1.1 History	18
2.1.2 General Properties	19
2.1.3 General Applications	21
2.2 Bi-layer Structure Ceramics	23
2.3 Pore-forming Agents	24
2.3.1 Nano Carbon Black	24
2.3.2 Polypropylene	26
2.3.3 Poly (methyl methacrylate)	27
2.4 Porous ceramic	28
2.4.1 Material of Porous Ceramics	29
2.4.2 Characterization of Powders	30
2.4.3 Performance of Ceramics	34
2.5 Concluding Remaks	36

CHAPTER 3	METHODOLOGY	37
3.1	Introduction	37
3.2	Raw Materials	37
3.2.1	Clay	37
3.2.2	Feldspar	39
3.2.3	Silica	40
3.3	Design of Experimental	42
3.3.1	Parameters For Raw Materials	43
3.3.2	Parameters of Sintering	44
3.4	Fabrication of Porous Ceramic	46
3.4.1	Weight and Mixing	46
3.4.2	Sieving	48
3.4.3	Pressing	50
3.4.4	Sintering	52
3.5	Testing of Powder and Ceramic	53
3.5.1	Density and Porosity (Archimedes Principle)	53
3.5.2	Rockwell Hardness Test	54
3.5.3	XRD Test	56
3.5.4	Scanning Electron Microscope (SEM)	57
CHAPTER 4		59
4.1	Introduction	59
4.2	Rockwell Hardness Test	59
4.3	Porosity/Density (Archimedes Principle)	63
4.4	Scanning Electron Microscope	67
4.5	X-Ray Diffraction analysis	68
CHAPTER 5		70
5.1	Conclusion	70
5.2	Recommendation	71
REFERENCES		72
APPENDICES		76

LIST OF TABLES

TABLE	TITLE	PAGE
Table 3.1:	Weight of Raw Material Powder	46
Table 4.1:	Result for Rockwell Hardness Test	60
Table 4.2:	Result of Apparent Porosity for 1150°C	64
Table 4.3:	Result of Apparent Porosity for 1200°C	65



LIST OF FIGURES

FIGURE	TITLE	PAGE
Figure 2.1:	Example of Ceramics	19
Figure 2.2:	Characteristic ceramic atom	21
Figure 2.3:	Ceramic grinding wheel	22
Figure 2.4:	Examples of clay products	23
Figure 2.5:	Optical micrograph of poppy seed	32
Figure 2.6:	Optical micrograph of lycopodium spores	33
Figure 2.7:	Particle size distribution of the lycopodium powder	34
Figure 3.1:	Example of clays	38
Figure 3.2:	Example of Feldspar	39
Figure 3.3:	Example of Silica powder	41
Figure 3.4:	Flowchart of preparation and fabrication of ceramic	42
Figure 3.5:	Calculation Weight Material	43
Figure 3.6:	Sintering Temperature Profile for 1150 °C	44
Figure 3.7:	Sintering Temperature Profile 1200 °C	45
Figure 3.8:	Sintering Temperature Profile 1250 °C	45
Figure 3.9:	30 Balls Milling mix with powder	47
Figure 3.10:	Ball Milling machine	47
Figure 3.11:	Sieving Process	48
Figure 3.12:	Result Powder after Sieving for 0%wt	48
Figure 3.13:	Result Powder after Sieving for 3%wt	49
Figure 3.14:	Result Powder after Sieving for 5%wt	49

Figure 3.15: Result Powder after Sieving for 10% wt	49
Figure 3.16: SM100-Universal Test Machine	50
Figure 3.17: Mould for Porous Ceramic Powder Pressing	51
Figure 3.18: Pressing Process	51
Figure 3.19: Compact Powder after Pressing	51
Figure 3.20: Heat Treatment Furnace machine	52
Figure 3.21: Densified Porous Ceramic samples	53
Figure 3.22: A&D FZ-300i-EC Precision Balance	54
Figure 3.23: Laboratory Archimedes setup	54
Figure 3.24: Mitutoyo HR-400 Hardness Tester	56
Figure 3.25: Diamond Ball Indenter	56
Figure 3.26: ZEISS EVO 18 model	58
Figure 4.1: Hardness Test	59
Figure 4.2: Result of Rockwell Hardness Test for 1150°C	60
Figure 4.3: Result of Rockwell Hardness Test for 1200°C	61
Figure 4.4: Archimedes Principle	63
Figure 4.5: Result of Apparent Porosity for 1150°C	65
Figure 4.6: Result of Apparent Porosity for 1200°C	66
Figure 4.7: SEM characterizat on of sintered discs produce with nano-carbon black as pore forming agent	67
Figure 4.8: SEM characterizat on of sintered discs produce with nano-carbon black as pore forming agent	68
Figure 4.9: Porous ceramic diffraction pattern on 0wt% nano carbon black content	69



اونيورسيتي تيكنيكل مليسيا ملاك

UNIVERSITI TEKNIKAL MALAYSIA MELAKA

LIST OF SYMBOLS AND ABBREVIATIONS

D,d	-	Diameter
°C	-	Celcius
W	-	Weight
wt%	-	Weight Percentage
μm	-	Micron
MPa	-	Megapascal
g/cm ³	-	Grams per cubic centimeter
N/mm ²	-	Newton per square millimeter



LIST OF APPENDICES

APPENDIX	TITLE	PAGE
APPENDIX A:	GANTT CHART PSM 1	76
APPENDIX B:	GANTT CHART PSM 2	77
APPENDIX C:	XRD Result 0wt% Nano-carbon black	78
APPENDIX D:	XRD Result for Aluminium Oxide	80
APPENDIX E:	XRD Results of Potassium Oxide	82
APPENDIX F:	XRD Results for Silicon Oxide	83



CHAPTER 1

INTRODUCTION

1.1 Research Background

Technical function becomes extremely crucial in human-occupied projects where thermal comfort is required. As a result, we can confirm that ceramic tiles do not provide enough thermal comfort in many instances.

The human body may be thought of as a thermal machine that creates between 100 and 1000 W of heat depending on the activity done. The heat created by the human body must be dispersed in order to maintain a consistent body temperature (normally between 35 and 37 °C). Thermal regulator mechanisms are in charge of this. Many aspects that contribute to comfort are described by an individual's physiological and psychological reaction intensities to the environment (Effting et al., 2007). The main environmental variables are air temperature, relative humidity, wind speed and radiant temperature (Resources, 2017).

The ceramic manufacturing is continually pursuing market amplification for the sector, as well as enhancing product quality and extending the variety of behaviors performed. The concept of producing ceramic surfaces that give thermal comfort to the person aids market sectors that have been rarely explored, such as hot situations such as swimming pool areas and cold environments such as bedrooms and baths.

Porous inclusion can provide materials with low conductivities and densities. Generally, thermal conductivity of porous materials decreases as porosity increases (Science, 1975). The porosity of ceramic materials is often related to the processing parameters used. High porosity, on the other hand, often signifies inferior mechanical strength. By properly mixing raw materials and processing methods, porous ceramics with good mechanical strength and chemical resistance may be manufactured. It is also possible to obtain exceptional refractoriness and structural uniformity, as well as favourable thermal qualities for a specified application.

Porous ceramics may be manufactured in a variety of ways. Incorporation of organic compounds in the ceramic body that are later removed during the firing stage was an early technology that is still widely used today. Other techniques offer significant advantages and may be used in the future. Processing control and, as a result, final material properties are a rampant problem.

1.2 Problem Statement

Thermal properties of ceramic materials are heat capacity, thermal expansion coefficient, and thermal conductivity. A solid can either store or convey thermal energy. Heat capacity is a material's ability to absorb heat from its surroundings. This demonstrates that the major reasons why the surfaces of ceramics were at high temperatures when exposed to external surroundings that are exposed to solar radiation.

It is possible to manage the porosity of ceramic tiles by adding pore-forming agents, which eventually helps to reduce heat conductivity. The existence of pores, in general, can have a negative impact on mechanical strength. As a result, to reduce heat conductive ceramic without sacrificing mechanical strength.

Pore-forming agents, in particular, have demonstrated the ability to achieve high porosity levels. Organic particles are burned off during the heating process to the firing temperature, producing voids in the ceramic body. The shape of these voids will be determined by the pore-forming agent used, and may thus be regulated by appropriate incorporation content and particle size distribution.

Despite the fact that starch is the most commonly used pore forming agent, potentially due to its biological origin and availability, the struggles in trying to maintain the pore structure developed by the starch burn out, and the limited size range of commonly produced starch types (typically between 5 and 50 μm) limit its application when large pores are intended (Živcová et al., 2007).

Three different pore-forming agents will be using namely Nano Carbon Black (NCB). Nano Carbon Blacks were preferred because their large scale manufacturing and low cost, making them economically advantageous for industrial applications.

As above mention, this research will focus on measure the performance of ceramic with different parameters by using pore agent Nano Carbon Black (NCB).

1.3 Research Objective

- a) To prepare and fabricate of ceramics with additional pore forming agent at various contents.
- b) To characterize of powders and ceramics using several analysis and testing.

1.4 Scope of Research

The study will be done in order to analyse the preparation of powder, fabricate of ceramics, characteristic of the powder or ceramic and study performance of ceramics. All this analysis will be done to achieve by the produce porous ceramic with low thermal conductivity for application and buildings.

There is a lot of type of powder to make ceramics, by studying the type of powder that we will be use is one of the steps in the preparation of powder. This preparation really importance because we need to choose the type of powder that help us to improve the low thermal conductivity of the ceramic that will be produced.

We will study or analyse the best forming method to fabricate the ceramics. There is some type of forming methods. Due to apparatus that have given in lab, we need to narrow down the type of forming agents that can be done. However, we still choose the method that will give a positive outcome to achieve the objective.

There are a few test and analysis that will be done such as X-ray diffraction analysis (XRD), Scanning Electron Machine (SCM), Three-point bending strength test and density porosity. All this test and analysis will be done to guide us to find the most suitable parameter or method that will be use. By gaining the result from the test and analysis, we can improve and fix the faulty.

Study performance of ceramics the most important steps to succeed our analysis. After finish the test, we will study performance of ceramics to acknowledge what is the porous ceramic demand to lower the thermal conductivity.

1.5 Significant of Study

The purpose of this study to understand the functionalities and properties of pore forming agent such as Nano Carbon Black (NCB), Polypropylene (PP) and Polymethyl methacrylate (PMMA) which become an agent that increase the porosity in ceramics.

The importance to understand the functionalities of the pore forming agent because, in general the pore forming agent can cause bad effect to ceramic. If the pore forming agent been using with incorrect parameters, it can cause ceramic has a large scale porosity. Furthermore, when the scale porous ceramic is higher, it can cause the ceramic has low mechanical strength. It will cause the ceramic will be easy to fracture.

In order to understand properly the properties of pore forming agent, we can control the porosity ceramic. Then, we can achieve to produce with perfect percentage of porosity ceramic that can help to improve the conductivity of heat. Which that is the main purpose of study to prepare ceramic with low thermal conductivity.

By doing this study, it's helping us to explore more analysis about the ceramic tile that's been used in the buildings. Due to sun radiation that cause external environment with high temperature, it will cause the ceramic surface to become hotter. The ceramic will absorb the heat from the environment and sun radiation. In this case, by understanding the functionalities and properties of pore forming agent can help to improve and solve this issue.

CHAPTER 2

LITERATURE REVIEW

2.1 Introduction

This chapter will explain about the previous studies being done on this topic which is structured ceramic. Generally, this chapter outlines the history, structure ceramic. This chapter presents the importance of reviewing previous studies and the advancement regarding the topic throughout the time. It is vital to do this in order to create an improvement on ceramic.

2.1.1 History

Ceramic tile has been utilized since the invention of clay roof coverings, many years ago, but it is still popular today, even though technical developments in tile have allowed it to be used on walls, floors, ceilings, fireplaces, murals, and even as external cladding.

Our English term 'ceramic' derives from the Greek word 'keramos,' which means 'pottery,' but its Sanskrit source means 'to burn.' This is due to the fact that the tiles were burnt in a hot oven to guarantee that they were sufficiently dry to survive the environment.



Figure 2.1: Example of Ceramics

While early tiles were baked in the sun, kilns were later used to harden the tile body and create a beautiful surface finish.

Architecture, traditions in ceramic tile, and subsequently, porcelain tile, have evolved over time to include not just ordinary roof tiles, but have also become decorative as well as practical. Brightly colored brick-and-tile panels have graced houses and public buildings from Spain to Turkey, while mosaic tiles were widely utilized in the Roman Empire, from the toilet to the dining room. Glazed ceramic plaque tiles were used in temples and shrines in Burma to narrate epic stories.

2.1.2 General Properties

The most essential general quality of ceramics is that they are refractory; they are rough-and-tumble materials that can withstand a great deal of damage in both ordinary and extreme circumstances. Consider this: most of us tile our kitchens and bathrooms because ceramic tiles are hard, waterproof, largely resistant to scratches, and maintain their appearance year after year; however, engineers also use very different ceramic tiles on space rockets to protect them from the heat when they return to Earth.

Ceramics are distinct from other materials. Their atoms are ionically bound, just like sodium and chlorine in sodium chloride, common salt, which keeps them securely in place, making ceramics hard and durable, and locks up all their electrons, so there are no free electrons to transfer heat or electricity, unlike metals. Metals are able to bend, flex, and be pulled into wires because their rows of regularly packed atoms move past one another. However, there are no rows of atoms in a ceramic; the atoms are either imprisoned in a regularly repeating three-dimensional crystal or randomly organised to form an amorphous solid, which is a solid that lacks a clean and tidy internal crystalline structure.

When you strike a lump of metal with a hammer, the mechanical energy you provide is wasted as layers of atoms leap past one another, causing the metal to bend out of shape. When you whack a ceramic, such as glass, there is nowhere for that energy to go; there is no way for the glass to bend and absorb the impact, so it shatters instead. This explains why ceramics are hard and fragile at the same time.

As we have seen, not all ceramics act in this manner. Graphite is soft because it is formed of layers of carbon atoms that slide and shear this is why a graphite pencil makes marks on paper, but diamond is hard because it has a considerably more solid crystalline structure. Clay is soft and malleable because, like graphite, its atoms are formed of flat sheets that may glide past one another, bound together only by weak connections. When water is added to clay, the polar water molecules (positively charged on one end and negatively charged on the other) assist to tear those bonds apart, making the clay even more pliable. When clay is burned, the water evaporates and the aluminium, silicon, and oxygen atoms lock into a stiff structure comprised of aluminium silicate, bound together by silicate glass, which is why fired clay is so hard (Chris Woodford, 2021).

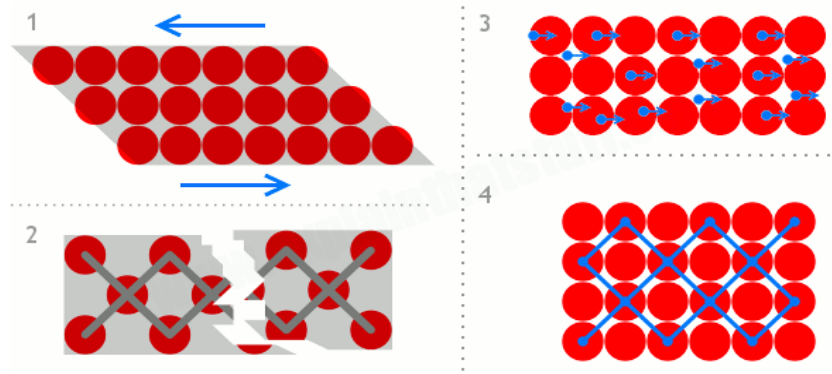


Figure 2.2: Characteristic ceramic atom

Ceramics have high melting temperatures, which makes them heat resistant, tremendous hardness and strength, significant resilience, which makes them long-lasting and hard-wearing, and poor electrical and thermal conductivity. They are good insulators and chemically inert, meaning they do not react with other compounds.

The porosity of a ceramic can influence its properties such as heat conductivity and hardness. This is owing to the low heat conductivity of the gaseous that fills the pore in the ceramic. As a result, the impact of thermal insulators in a ceramic is enhanced. Higher porosity, on the other hand, reduces its strength and durability. So, in order to remedy this problem, the porosity of the ceramic must be controlled.

2.1.3 General Applications

Ceramic materials used in engineering applications are classified into two types: conventional ceramics and engineering ceramics. Traditional ceramics are often comprised of three fundamental components: clay, silica (flint), and feldspar. Engineering ceramics, on the other hand, are made up of very pure compositions of aluminium oxide (Al_2O_3), silicon carbide (SiC), and silicon nitride (Si_3N_4).

Some ceramics are utilised as abrasive ceramics in industry. These are tools that are used to grind, wear, or chop away other materials. Thus, in addition to high toughness, the primary need for this class of materials is hardness or wear resistance. They must be refractorily since they may be subjected to extreme temperatures. Abrasive ceramic materials include diamond, silicon carbide, tungsten carbide, silica sand, and aluminium oxide/corundum.



Figure 2.3: Ceramic grinding wheel

Furthermore, certain ceramics are utilized clay products. One of the most common ceramic raw materials is clay. It is abundant and popular because to the simplicity with which items may be created. There are two types of clay goods: structural products and whitewares.



Figure 2.4: Examples of clay products

2.2 Bi-layer Structure Ceramics

Bi-layered ceramic tiles are made up of two layers with varying densities, are dense and porous, and have an adjustable thickness. The new manufacturing process consists of a double pressing action, which is quick and simple to use in the industrial setting and enables the establishment of a flawless interface bonding between layers. The bi-layered ceramic tile is made up of an upper layer with a density similar to that of a traditional porcelain stoneware tile and a porous bottom layer that facilitates weight reduction while keeping enough mechanical strength.

Because of its structure, this bi-layer structure has an advantage in ceramics. Thermal conductivity increases as porosity increases. The porosity of a ceramic can further reduce its thermal conductivity. However, increasing the porosity of a ceramic compromises its strength, rendering it unsuitable for structural applications. To address the issue, it is necessary to manage the ceramic creation process. By combining a bi-layer structure ceramic, the denser layer of the ceramic may overcome the poor strength of the ceramic due to porosity.

2.3 Pore-forming Agents

Porous ceramic materials are used in a variety of applications, including ceramic filters and membranes, fuel cell electrodes, catalytic supports for biomaterials, piezoelectric materials, and thermally or acoustically insulating bulk materials.

Several methods for producing porous ceramics have been documented. Pore-forming chemicals, in particular, have demonstrated the ability to achieve high porosity levels. Organic particles are burned off during the heating process to the firing temperature, producing voids in the ceramic body. The shape of these voids will be determined by the pore-forming agent used, and may thus be regulated by appropriate incorporation content and particle size distribution. Numerous pore-forming agents, including starch, graphite, Lycopodium, and polymethyl methacrylate, have been studied.

NCB (Nano carbon black) is the pore forming agent that will be used in this study. This performance agent was chosen because it has unique properties that aid to increase heat conductivity and mechanical strength.

2.3.1 Nano Carbon Black

Carbon black (CB) is a kind of carbon that arises in a controlled setting from the incomplete combustion and thermal degradation of gaseous or liquid hydrocarbons. This technique yields a fine, powdery black dust, which is one of the world's top 50 compounds. Carbon black is utilised as a filler in the rubber industry, but it is also an important component of many colours and inks. It is a conductive material that is used in the electrical sector to make electrodes and carbon brushes (Mylona, n.d, 2019)

Technical-grade carbon black is widely used in many industries as a technological ingredient, thermal insulator, thermostable material, and so on. Carbon black used in the tyre business is in the form of polydispersed granules 0.2-3.0 mm in size, which are generated in granulators from amorphous carbon black by the addition of a molasses-in-water binder solution containing 3 percent molasses by weight. The granules are then dried at temperatures ranging from 350 to 500°F. It is vital to know the effective thermal conductivity coefficient of such carbon black particles when estimating heat transfer processes in this and other processes (P. E. Khizhnyak, A. V. Chechetkin, 1980).

Carbon black is a porous and scattered substance. Given this, the effective thermal conductivity of carbon black must be understood as a value equal to the thermal conductivity of some homogeneous body, through which, given identical dimensions and temperatures on the boundaries, the same amount of heat passes as passes through the given carbon black.

The effective thermal conductivity of scattered and porous materials is widely known to be affected by the size and shape of the pores and cavities. A part of the pores and cavities may be closed volumes, while the remainder may link to form open channels. A variety of mechanisms cause heat transmission in such materials. Transfer happens via conductivity within the particles and at places of direct contact. Transfer happens in the pores and cavities' air medium due to both conductivity and radiation. The contribution of radiant heat transmission rises as pore and cavity size increases (P. E. Khizhnyak, A. V. Chechetkin, 1980).

The size of the cavities between particles increases with particle size, and the direct contact area between particles is bigger with coarser particles than with tiny particles. This

eventually results in a decrease in contact thermal resistance and, as a result, an increase in effective thermal conductivity.

2.3.2 Polypropylene

Polypropylene (PP), once found, was instantly praised for its extraordinary and diverse properties such as low density, the lowest of all thermoplastics, great chemical and corrosive resistance, dimensional stability, recyclability, flexibility, superior processability, and low cost. All of these benefits have led to its suitability for a wide range of applications and for processing via a variety of conversion processes (Hisham A. Maddah, 2016).

PP was chosen because of its large-scale manufacture and low cost, making it economically appealing for industrial uses. Previous research on the thermal breakdown of PP revealed that it decomposes into a vast variety of aliphatic molecules relatively quickly and with no long-term residue (Bockhorn et al., 1999). For PP no hazardous gaseous emissions are reported.

Furthermore, because to its superior processability, mechanical qualities, great chemical stability, and thermal stability, PP is considered as a suitable raw material for the manufacture of membranes. To far, PP has been widely used in the manufacture of porous membranes, mostly by thermally-induced phase separation and stretching method (Novais et al., 2014).

In terms of thermally-induced phase separation, PP and other components are firstly dissolved into a certain solvent to form the homogenous solution at high temperature, and the phase separation happens as the temperature decreases. Once the residual solvent is removed, the porous membrane is obtained (Dai et al., 2015).

For the stretching approach, the melting PP-based composite is treated to produce a precursor membrane with an orientated structure, and the precursor membrane is then stretched at low or high temperatures to induce the development of holes by lamella fracture or separation (Elias et al., 2000) The stretching technique has lately gained popularity due to its advantages such as ease of preparation, cheap cost, avoidance of solvent contamination and recovery, and so on. Many factors, including material and processing characteristics, have a significant impact on the pore development behaviour of PP membrane (Novais et al., 2014).

2.3.3 Poly (methyl methacrylate)

Poly (methyl methacrylate) is commonly utilised as a pore-forming agent in ceramics because it has an excellent balance of thermal characteristics that are appropriate for the application proposed (Novais et al., 2014). PMMA decomposes almost entirely to its monomer and burns at a rapid and consistent rate.

Poly (methyl methacrylate) (PMMA) is a transparent, synthetic and rigid polymer which presents low crystallinity as well as good mechanical strength and electrical properties. Among the applications of this polymer, it is important to highlight their use in parts for computers, fiber optics, 3D illuminated panels, solar deflectors, orthodontic equipment, among other purposes (Neumann MG, Schmitt CC et al, 2010). Thermal

analysis techniques were used to characterise PMMA nanocomposites. Researchers have previously explored the thermal stability of PMMA nanocomposites containing 3 wt% organoclay montmorillonite (Lerari et al., 2010). The results demonstrated that the organoclay may prevent the heat deterioration of PMMA. These findings are consistent with those reported by other researchers for PMMA with 10% C18 MMT organoclay. Another study looked at the thermal deterioration of PMMA with varied quantities of natural montmorillonite ranging from 2.5 to 15% by weight (Sahoo & Samal, 2007). According to the results the onset of thermal degradation for PMMA/MMT nanocomposites is higher when increasing the clay content.

2.4 Porous ceramic

Porous ceramics are defined as having a high proportion of porosity ranging from 20% to 95%. These materials are made up of at least two phases, such as a solid ceramic phase and a gas-filled porous phase (German et al., 2009). Because gas interaction with the environment is possible through pore channels, the gas content of these pores normally adjusts itself to the environment. Closed pores can hold a gas composition that is unaffected by the surroundings (Misyura, 2016).

When determining porosity for any ceramic body, porosity may be classified into two types: open accessible from the outside porosity and closed porosity. Open porosity is further subdivided into open dead-end pores and open pore channels. The existence of porosity depends on the individual application, thus a more open porosity, such as a closed porosity, may be required to be permeable, or a closed porosity, filters, or membrane, such as a thermal insulator, may be desired. The total porosity is defined as the sum of open and

closed porosity. When a material's fractional porosity is low, the closed porosity dominates; as the fractional porosity grows, the open porosity level increases.

Porous ceramics have been classed based on the kind of porosity, volume percentage, and size of the pores (Gaydardzhiev et al., 2008) The nature of porosity in natural ceramics is determined by their origin, but in synthetic ceramics, it is determined by production and, in general, it may be regulated. These materials' pore sizes may be divided into three categories based on pore diameter: microporous (less than 2 nm), mesoporous (between 2 and 50 nm), and macroporous (more than 50 nm) (more than 50 nm). Typically, the pore size distributions are measured using the mercury intrusion porosimetry method. The pore size distribution of the closed porosity cannot be determined using this approach, but it may occur through optical and electronic analysis of a polished cross section, for example. The pore size distribution describes the pore volume as a function of pore size and is often expressed as a percentage or a derivative (Nimmo, 2013).

2.4.1 Material of Porous Ceramics

One of the most essential factors is the material used to create porous ceramic. All of these materials are used to manage the porosity scale in ceramic to generate an excellent porous ceramic product.

As a result, the fabrication of porous ceramics with regulated microstructure porosity, pore size, and pore space topology has been a consistent focus of research over the last few decades. Sol–gel techniques for pores in the nanometer size range and extremely high porosity, the use of polymeric foam templates for large pores and extremely

high porosity, biomimetic processing such as pyrolyzed wood templates, ceramic hollow spheres such as alumina microballons. These are all common processing methods. and sacrificial (pyrolyzable) poreforming agents (PFA), which are synthetic organics or natural biopolymers that burn off during the firing process (Rice, 1996).

Although many other PFA have been suggested and employed in ceramic technology, such as carbon, poly-vinyl-chloride, polystyrene, wood flour saw dust, and crushed nut shells, it appears that starch, a natural biopolymer composed of amylose and amylopectin, has risen to prominence as a PFA today (Mattern et al., 2004) including its most recent use as a pore-forming and body-forming ingredient in starch consolidation casting.

The lack of hygiene and environmental concerns, easy handling and processing including defect-free burnout, the easy commercial availability in arbitrary amounts, at low cost and with constant, controlled quality, the rounded shape with well-defined aspect ratio usually close to unity, without large scatter, and the welldefined size distribution for each starch type are among the main reasons for starch's success as a PFA in ceramics (Živcová et al., 2007).

2.4.2 Characterization of Powders

As previously stated, starch may act as a body-forming agent in starch consolidation casting due to its capacity to swell in water at increased temperatures, allowing ceramic green bodies to be created by slip casting suspensions containing starch into nonporous moulds such as metal moulds.

Unfortunately, the pore size range achieved by using different starch kinds as PFA spans only around one order of magnitude below 100 μm median diameters between 5 and 50 μm for rice and potato starch, respectively (Gregorová & Pabst, 2007). It should be highlighted that this pore size range, which is very closely related to the initial size of the starch granules, relates to the pore diameter proper, which may be determined using 3D tomography or microscopic image analysis, for example. The pore size measured by mercury intrusion, on the other hand, relates to the pore throat size, or the size of the interconnections between open pores, and is often considerably smaller, on the order of magnitude 1–10 μm . Larger pore sizes are clearly desirable for various reasons, such as thermally or acoustically insulating materials, large-scale lightweight ceramics, or the ingrowth of bone tissue into bioceramic implant materials, in the latter instance of course associated with a high degree of interconnectivity.

In this regard, blue poppy *Papaver rhoeas* L. seed, a natural product of biological origin and a well-known raw material in the food business, might be a viable PFA for ceramics. The findings indicated that poppy seed is a viable pore-forming agent for ceramics. In this concentration, defect-free burnout was achievable using a standard firing plan without the requirement for a particular heating schedule to burn off the organics. The most intriguing aspects of employing poppy seed are its relatively big size (about 1 mm) and the fact that its density is similar to, but somewhat higher than, that of water. As a result, poppy seed suspensions are quite simple to make, whereas many other PFAs with lesser density, such as synthetic polymers and ceramic microballoons, would display severe buoyancy effects at this scale. A hierarchical pore structure is formed when potato starch is combined with a PFA that is more than one order of magnitude smaller (Gregorová & Pabst, 2007).

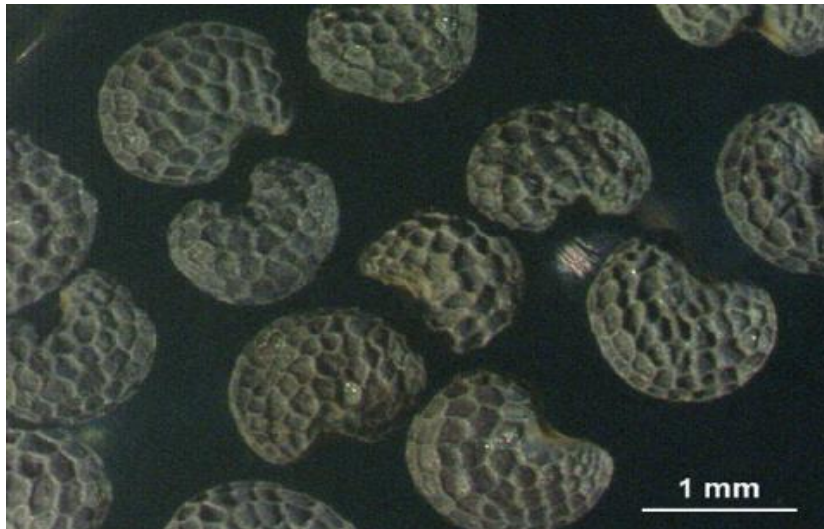


Figure 2.5: Optical micrograph of poppy seed

Furthermore, lycopodium spores have been identified as a novel PFA for the manufacture of porous alumina ceramics. Lycopodium spores may be easily combined with ceramic solutions, demonstrate excellent rheological behaviour up to a specific concentration, and result in a homogeneous microstructure with isometric holes somewhat smaller than 30 μm in size and a percolation threshold slightly higher than 10%. The researcher would like to underline that the filtering performance indicated above is governed principally by the interconnections between the pores in the sintered ceramic, which extend practically to the submicron range. As a result, the materials in this study will have high fine particle retention (Adler, 2005). As a result, they might be candidates for particle filters.

Lycopodium powder for this work supplied by H. Klenk, Schwebheim, consists of isometrically formed spores of several club mosses and ground pines, including *Lycopodium clavatum* L. (Wilder, 1970). The particle size distribution was determined by manual sampling of 1,000 spores and laser diffraction (Analysette 22 NanoTec, Fritsch, Idar-Oberstein, Germany) using the Fraunhofer approximation and microscopic image

analysis (Jenapol, Zeiss, Jena, Germany and Lucia G 4.81, Laboratory Imaging, Prague, Czech Republic). After changing the number-weighted distribution to a volume-weighted distribution, the median diameter is 30.6 μm according to laser diffraction and 33.1 μm according to image analysis. Obviously, the explanation for the little discrepancy is the presence of spore pieces and dust with a size smaller than 20 μm , which was overlooked in the picture analysis. The size distribution of the spores is relatively narrow, indicating that the natural development circumstances in this case result in very monodisperse systems. This is, of course, advantageous in terms of pore size controllability in porous ceramics (Gregorová & Pabst, 2007).



Figure 2.6: Optical micrograph of lycopodium spores

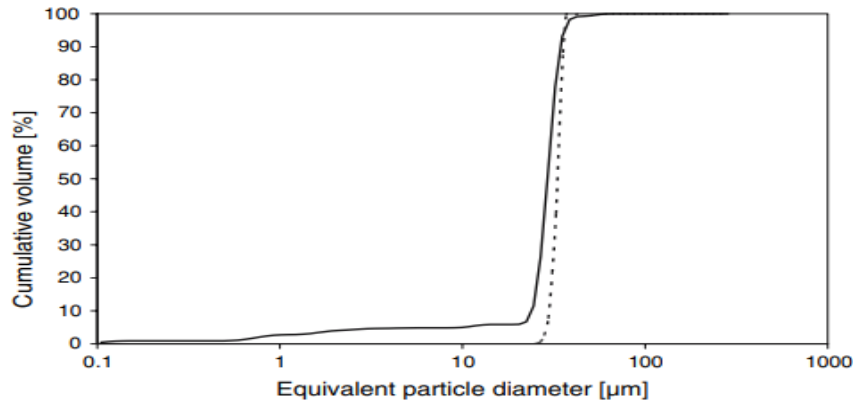


Figure 2.7: Particle size distribution of the lycopodium powder

2.4.3 Performance of Ceramics

The outcome for poppy seed (blue poppy seed, made by RH natur s.r.o., Uhersice, Czech Republic) with its typical spherical kidney-like form and fine polygonal network pattern on the surface. The size range is fairly restricted. The greatest Feret diameter was $1265 \pm 78 \mu\text{m}$, the minimum Feret diameter was $1038 \pm 68 \mu\text{m}$, and the aspect ratio was 1.22 ± 0.07 , according to microscopic image analysis. These data show that the divergence from spherical form is statistically significant but not huge, not too far from unity. The density of poppy seed does not appear to be documented in the literature. As a result, for the current study, it was assessed by floating in a sugar solution (saccharose), sugar was added to the water in which the poppy seed had sunk down until the poppy seed displayed buoyancy, and the density was determined to be $1.10 \pm 0.05 \text{ g/cm}^3$. This value must be known in order to manage the volume concentration of PFA in the system.

Z. Zivcova' E. Gregorova' W. Pabst analysis for lycopodium powder (2007).

Because of their monodispersity (narrow particle size distribution), lycopodium powder systems are excellent options for pore-forming agents that may efficiently regulate pore

size in porous ceramics. Thermal study shows that the burnout behaviour of lycopodium spores is comparable to starch, and it has been shown in this work that it does not cause any issues in high-temperature processing. Of course, when slip casting is utilised to shape the green bodies, the rheology must be properly regulated. This, of course, necessitates decreasing the alumina concentration in the suspension at the expense of increased shrinkage depending on the required amount of pore-forming agent and currently restricts the lycopodium content to values less than 40 vol.%. Although the fluidity of the system is satisfactory when the alumina content is reduced to 68 wt% at this concentration, The resultant ceramic bodies have large porosity gradients, with a greater lycopodium content resulting in increased porosity in the middle and an almost lycopodium free thick after-firing surface layer. However, it is envisaged that these challenges may be handled by optimising lycopodium dispersion at greater lycopodium concentrations by management of the mutual contact forces, utilising suitable deflocculants. As a result, porous ceramics with up to 50% porosity and a homogeneous microstructure consisting of around 30 μm pores appear to be a feasible aim for the near future. As a result, lycopodium is a good choice for filling the gap in PFA diameters and pore sizes left by commercially available starch varieties (Gregorová & Pabst, 2007). As a consequence of this research, it has been demonstrated that combining lycopodium spores with other pore-forming agents such as starch may be a feasible way to alter the ratio of open and closed porosity while maintaining the same degree of overall porosity.

2.5 Concluding Remarks

This chapter has covered broad characteristics and applications, but the major purpose of this chapter is to understand the characterisation of powders and porous ceramics that have been influenced by various pore producing agents from prior research. This general chapter aids in understanding the role of pore producing agents in porous ceramics. Furthermore, aid in the investigation of ways to increase the thermal conductivity and strength of porous ceramics.



CHAPTER 3

METHODOLOGY

3.1 Introduction

This chapter will discuss three key subtopics, the first of which is an explanation of raw materials. The following subtopic will discuss experimental design and fabrication, and the final subtopic will discuss the explanation of analytical characterisation.

3.2 Raw Materials

To create porous ceramic samples, four different types of raw materials are used. Clay, feldspar, silica, and a pore forming agent will be used as raw materials.

3.2.1 Clay

The term "clay" is used in a variety of contexts. It is a geological term that refers to a naturally occurring, earthy, fine-grained substance that displays flexibility when combined with a small amount of water. Additionally, it is a particle size phrase that has been long used in the examination of sedimentary rocks and soils, referring to particles larger than 2 μ m. This limit represents a natural division between clay minerals, which typically exist as particles of 2 μ m in diameter, and non-clay minerals, which occur in larger particles. Between roughly 1930 and 1960, the clay mineral notion proposed in the 1920s and 1930s that the clay fraction of a soil or rock is composed of microscopic particles of a restricted number of crystalline minerals was verified. The minerals were found and their

structures characterised utilising cutting-edge research techniques at the time (Brindley et al., 1981).

Clay minerals are widely used as inert fillers in polymers, paints, and the paper industry, their value derived from their ability to substitute for more expensive ingredients or from their physical usefulness (arising from the anisotropic particle shape). Clay minerals, on the other hand, are chemically reactive. Their application in ceramics, for example, is motivated by phase transitions and intercrystal reactivity. Additionally, clay minerals are utilised to synthesise zeolites for ion exchange, catalysts, and catalyst supports. They have even been implicated in the origin of life by forming complex organic molecules via catalytic surface creation. Finally, while clays are typically found in nature, they can be synthesised synthetically using certain ionic substitution patterns. Certain of these materials are used as rheology modifiers, for example. (Brindley et al., 1981)



Figure 3.1: Example of clays

3.2.2 Feldspar

Feldspar is by far the most prevalent mineral group in the earth's crust, accounting for around 60% of terrestrial rocks. The majority of deposits contain sodium feldspar, potassium feldspar, and mixed feldspars. Due to their high alumina and alkali content, feldspars are predominantly used in industrial applications. The term feldspar refers to a wide variety of materials. The majority of the things we use on a daily basis are composed of feldspar: glass for drinking, glass for protection, fibreglass for insulation, bathroom floor tiles and shower basins, and dinnerware. Feldspar is a mineral that we encounter on a regular basis.

Feldspar is the second most essential element in the creation of ceramics, behind clay. Feldspar lacks a defined melting point, as it melts gradually across a wide temperature range. This significantly simplifies the melting of quartz and clays and, with suitable mixing, provides for modulation of this critical step in ceramic production. Feldspars are employed as fluxing agents at low temperatures to create a glassy phase and as a source of alkalies and alumina in glazes. They enhance the ceramic body's strength, toughness, and durability, as well as cement the crystalline phase of other ingredients by softening, melting, and wetting other batch constituents.



Figure 3.2: Example of Feldspar

3.2.3 Silica

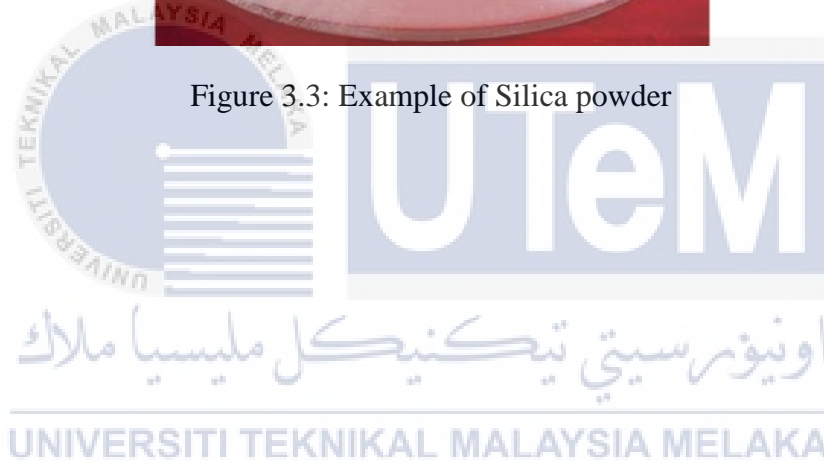
Silica is formed of silicon dioxide as a mineral. Silicon dioxide (as quartz mineral) almost always exists in the body in the form of unmelted particles embedded in the fired matrix (although finer one dissolve into the inter-particle glass). However, in glazing chemistry, we are discussing silica, the oxide. Silicon dioxide, the oxide, is present in all glazes that melt fully and re-solidify. Many are 70% or above. As kiln temperatures rise, materials release their silicon dioxide into the glaze melt. At various temperatures, different materials dissolve into the melt. The particle size of the components has an effect on how quickly they dissolve in the melt. Silicon dioxide is the primary glass-forming ingredient in glazes. Silicon dioxide can combine with virtually any other oxide to form a glass structure.

Silica is required for the manufacture of ceramics and refractories. Silica silicon dioxide is used in the creation of ceramics to assist control thermal expansion, regulate drying and shrinkage, and improve structural integrity and aesthetics. Silica is required for the glazing of products such as tableware, sanitary ware, and floor and wall tiles, as well as their body composition. Silica forms the skeletal structure of the ceramic body, which clays and flux components adhere to. Apart from skeletal formulation, Silica is frequently used to modify the qualities of other products in order to boost their heat stability, durability, and even pigment extension, hence lowering demand for expensive pigments such as titanium dioxide. Ceramics made with silicon dioxide have improved performance in terms of brightness, reflectance, colour uniformity, and oil absorption.

Additionally, silica materials are employed as primary aggregates in the manufacture of shaped and monolithic refractories. In high-temperature environments such as industrial furnaces, the silica gives resistance to acidic assault. Silica enables ceramics and refractories to preserve their critical properties at a cheaper cost while delivering additional benefits to their manufacturers.



Figure 3.3: Example of Silica powder



3.3 Design of Experimental

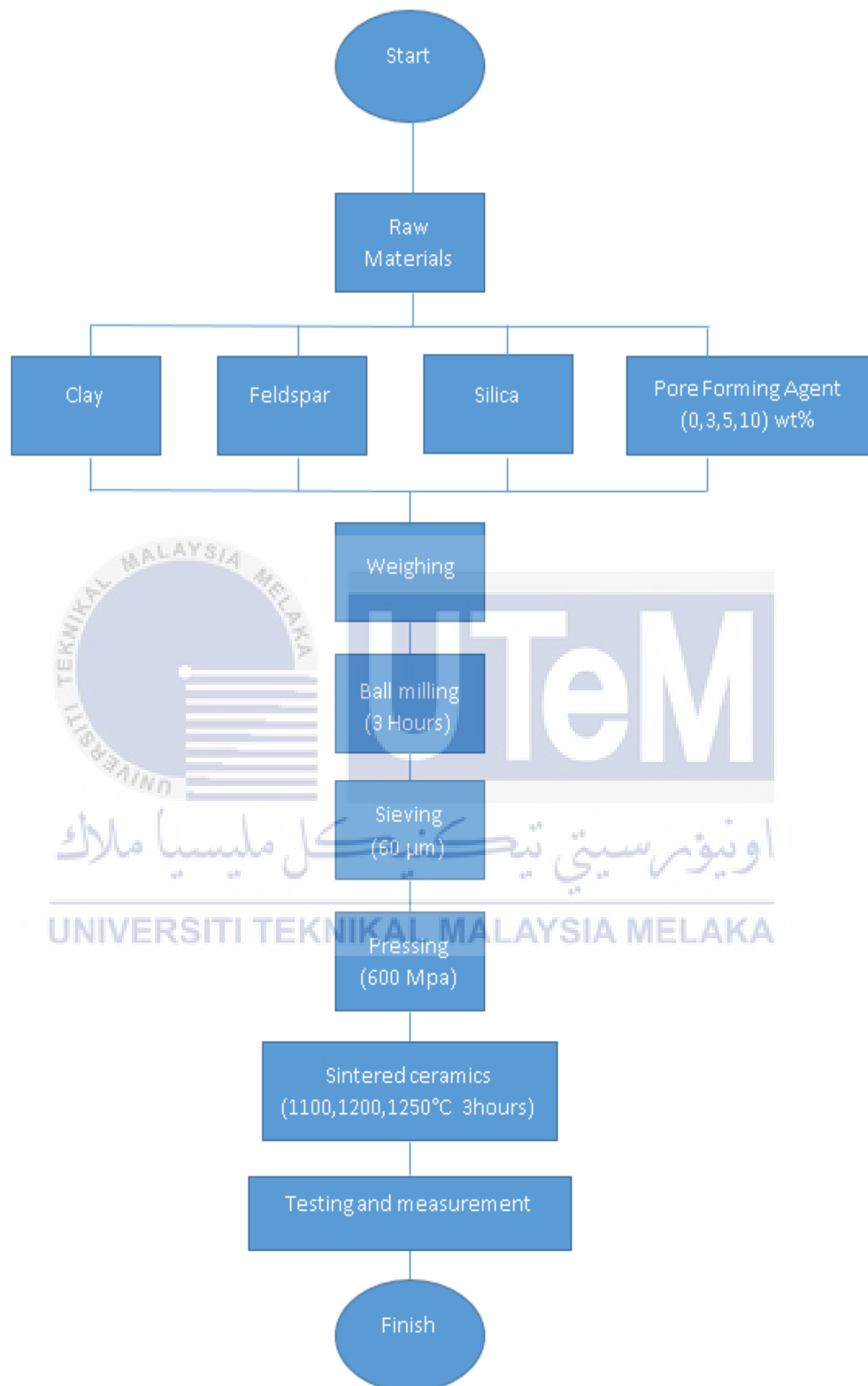


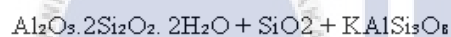
Figure 3.4: Flowchart of preparation and fabrication of ceramic

3.3.1 Parameters For Raw Materials

The sample ceramic mixture is produce using clay (kaolinite), silica (silicon dioxide) and feldspar (microcline). This mixture of porosity ceramic can define chemical equation to $\text{Al}_2\text{O}_3 \cdot 2\text{Si}_2\text{O}_2 \cdot 2\text{H}_2\text{O} + \text{SiO}_2 + \text{KAlSi}_3\text{O}_8$. Based on chemical equation can calculate the total weight of composition to 310g. Therefore, can be calculate each material weight based of the total weight of the composition. Refer to diagram 3.3.1, the weight for clay 24.84g, feldspar 40.64g and silica 4.51g.

Calculation weight material:

Clay (kaolinite) + Silica (silicon dioxide) + Feldspar (microcline)



$$= [2(13) + 3(8) + 2(14+16) + 2(2+8)] + [16+16] + [19+13+52+64]$$

$$= 310g$$

$$\frac{\text{Clay}}{\text{Clay} + \text{Feldspar} + \text{Silica}} \times 70g$$

$$\text{Clay} = \frac{110}{310} \times 70g = 24.84g$$

$$\text{Feldspar} = \frac{180}{310} \times 70g = 40.64g$$

$$\text{Silica} = \frac{20}{310} \times 70g = 4.51g$$

Figure 3.5: Calculation Weight Material

3.3.2 Parameters of Sintering

Sintering process involves in the fabrication of the structure sample. This cycle of sintering one of the crucial part to produce densified porous ceramic. In this research, the compact powder will be partially sintered by firing at 1150, 1200 and 1250°C. These temperatures will proceed base on single ramp-up sintering temperature profile. Each of the temperature will increase 5°C/min until reach sintering temperature and cooling down naturally which depends on room temperature, normally 25-28°C. This pre-heat phase setup is allowing the compact porous ceramic to get oxidized before powder consolidation. By that, the sample can be secured from bursting out the structure.

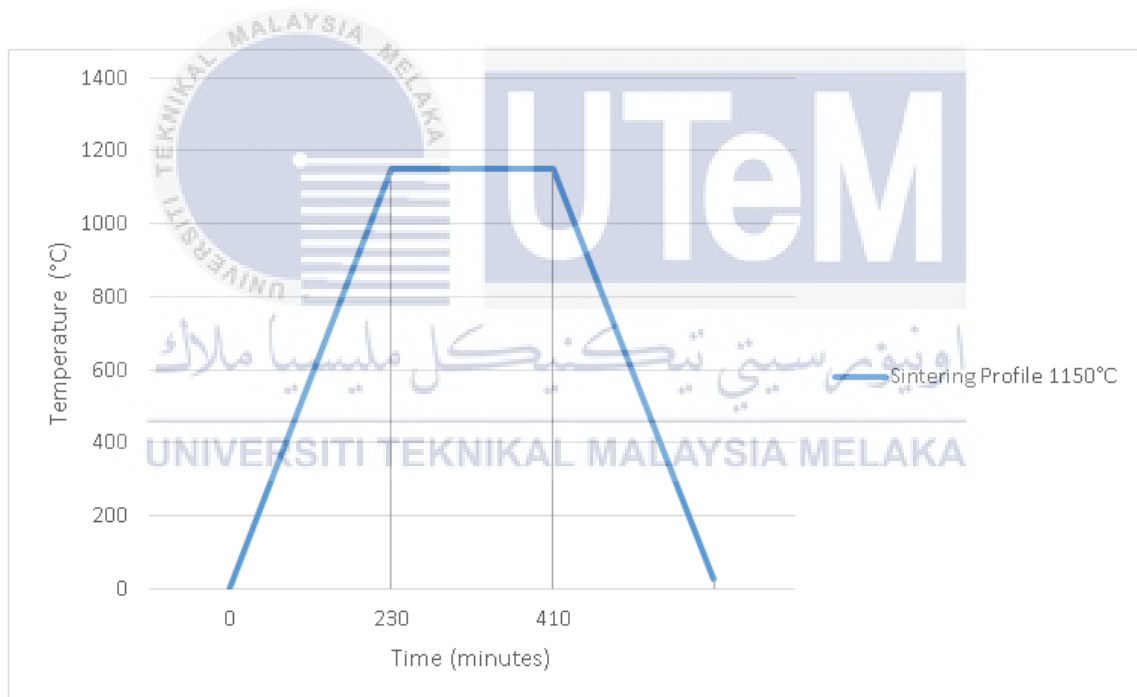


Figure 3.6: Sintering Temperature Profile for 1150 °C

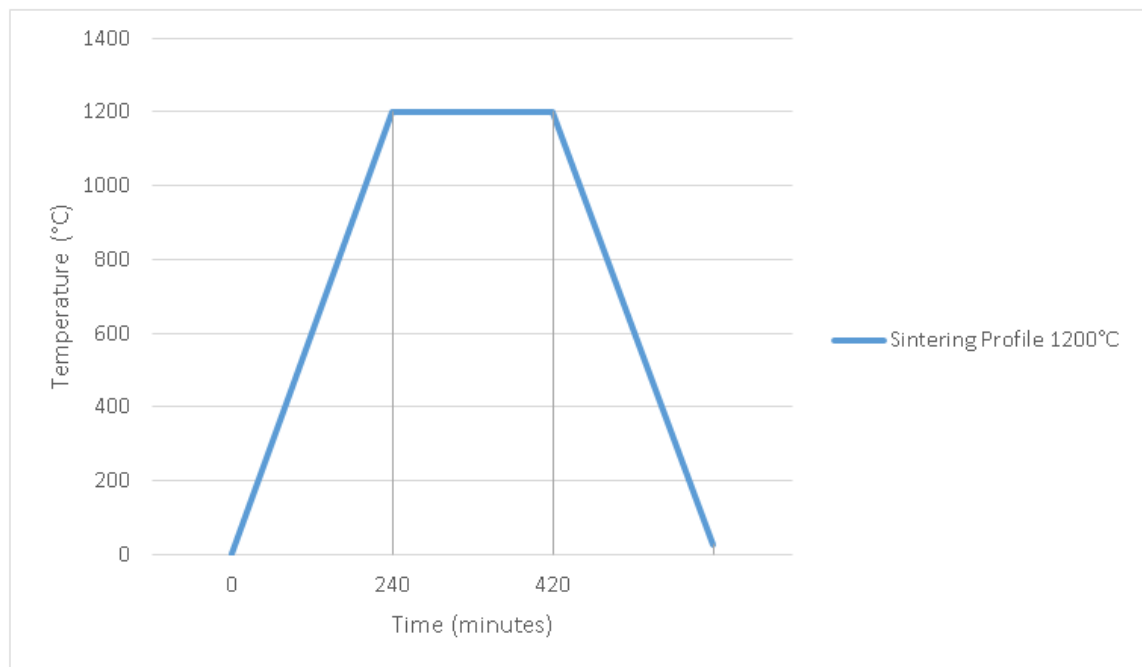


Figure 3.7: Sintering Temperature Profile 1200 °C

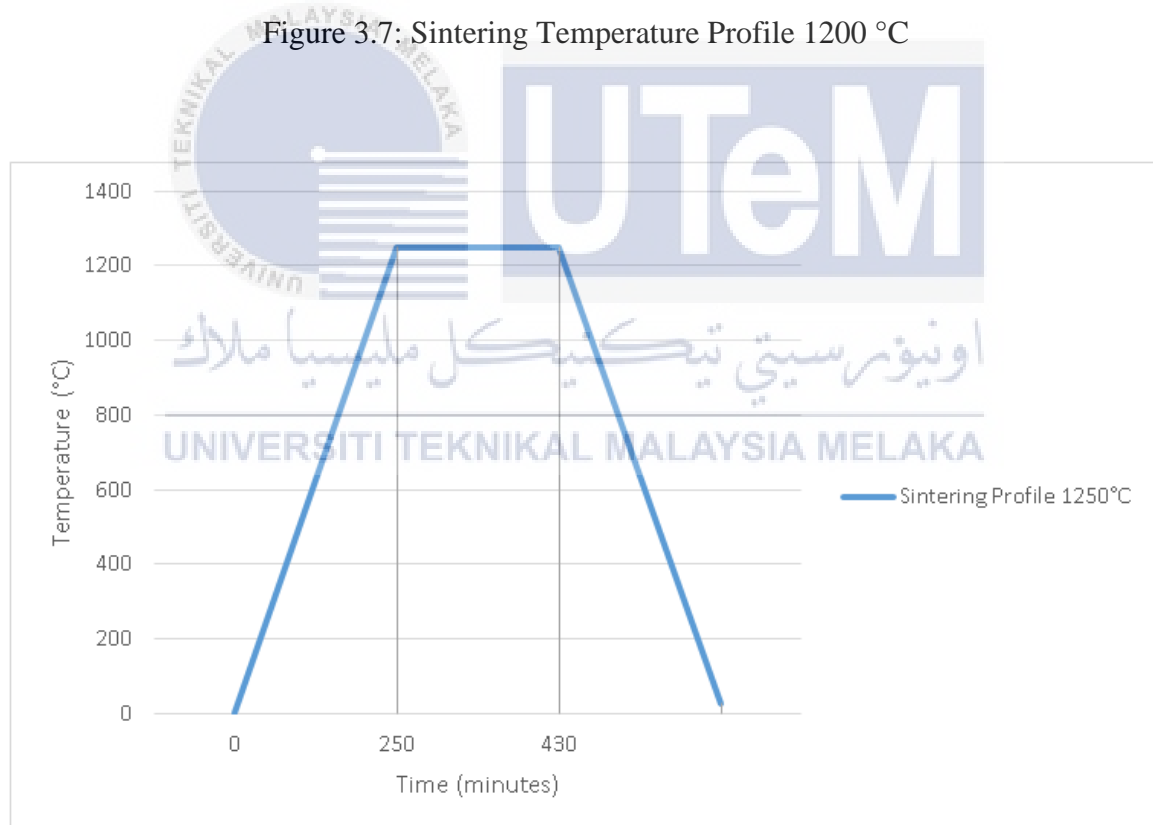


Figure 3.8: Sintering Temperature Profile 1250 °C

3.4 Fabrication of Porous Ceramic

The fabrication of ceramic structure sample will be in the thin circular disc. The sizing of the cylinder will be in the diameter of 11mm and average thickness of 4mm. There will be 4 different type mixture of ceramic which is in the ratio of 0,3,5 and 10% weightage of 70g. From every type of sample there will be produce into 12pieces of ceramic. Therefore, the total sample that produce will be 48pieces ceramic. Every type ratio mixture produces 12pieces for testing purpose.

3.4.1 Weight and Mixing

Every raw material powder been weight based on calculation. This weight process to ensure each of the sample have a stable amount of percentage raw powder in the porous ceramic composition. After that, the composition will be added porous ceramic agent by categorization of 0,3,5,10 wt% as shown table below:

Table 3.1: Weight of Raw Material Powder

	clay	Feldspar	Silica	Sodium Silicate	Nano-Carbon Black
0%	24.48g	40.64g	4.51g	5g	0g
3%	24.48g	40.64g	4.51g	5g	2.1g
5%	24.48g	40.64g	4.51g	5g	3.5g
10%	24.48g	40.64g	4.51g	5g	7g

After that, the powder composite of porous ceramic will be mixing by using ball milling. Ball milling is a mechanism of grinding composite powder into extremely fine powders. Every porous ceramic powders will be mixing with ball mill machine for 3hours with a consistent rotational speed. Meanwhile for the ball milling, 30 milling balls were put in the jar with porous ceramic powder to help the mixing process more efficient.



Figure 3.9: 30 Balls Milling mix with powder



Figure 3.10: Ball Milling machine

3.4.2 Sieving

After mixing process some granulate powder occur, by that sieving process is needed to do next. Sieving process help to separated bigger particles to smaller particle size distribution of a sample. Sieving is performed to separate the powder sample with 60 μ m particle size by submitting it to mechanical force. The sample will be moved either in vertical or horizontal direction and the movement will superimpose in tap sieve shakers.



Figure 3.11: Sieving Process



Figure 3.12: Result Powder after Sieving for 0% wt



Figure 3.13: Result Powder after Sieving for 3% wt



Figure 3.14: Result Powder after Sieveing for 5% wt



Figure 3.15: Result Powder after Sieving for 10% wt

3.4.3 Pressing

As mentioned before, the fabrication of the ceramic structure sample will be in the thin circular disc. Thin circular disk one of the simple form and size known to successfully compact the powder in a uniform density under a uniaxial charge. The dimensioning of the cylinder will be in the diameter of 11mm and the average thickness of 4mm. This form requires a small amount of material used relative to the square form of the tile. To manufacture the porous ceramic structure in this method which are using the SM100-Universal Test Machine. The process started with adding the porous ceramic powder into the cylinder shape mould (based on figure 3.4.3.1) and push the plunger towards the sample powder with low amount of pressure in order to form an initial compact. Next, install the mould into the universal test machine and start pressing at 600 MPa for 60 seconds. The powder will become disk-shaped, structure with acceptable force. This shows that dry pressing is one of the most important processes as the determination of the sample force.

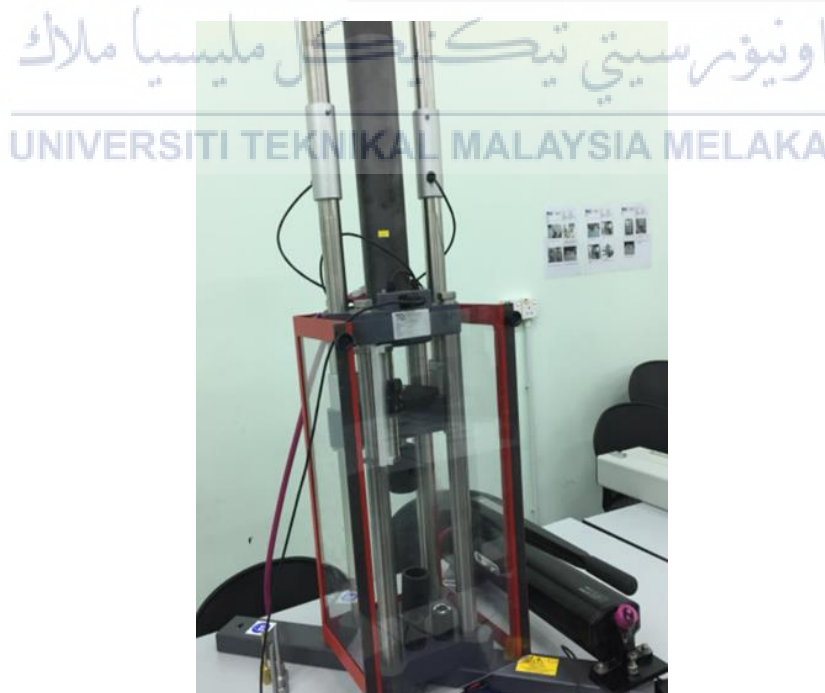


Figure 3.16: SM100-Universal Test Machine



Figure 3.17: Mould for Porous Ceramic Powder Pressing

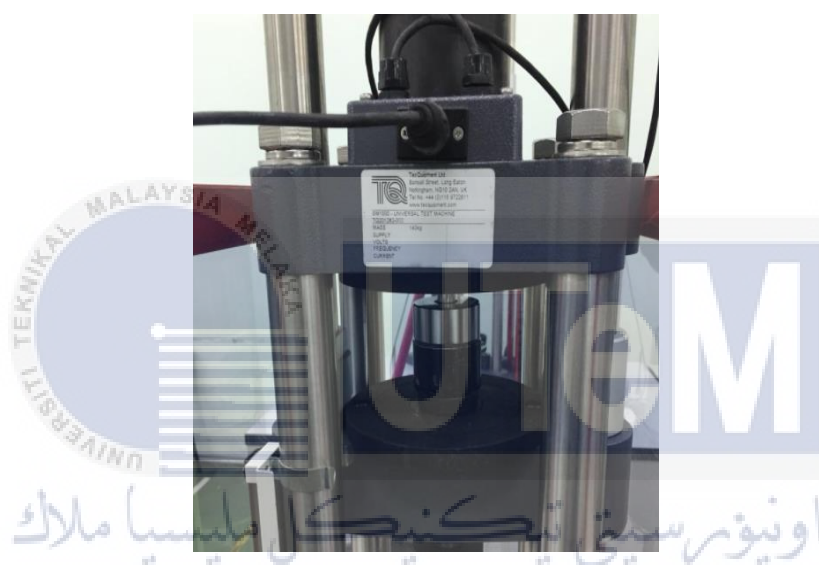


Figure 3.18: Pressing Process



Figure 3.19: Compact Powder after Pressing

3.4.4 Sintering

After pressing, sintering process should be done to help the compact porous ceramic powder become a densified ceramic. Sintering process by firing the porous ceramic material to solidifying the ceramic powder particles by heating the "green" compact to a temperature below the melting point as the material of the individual particles diffuses into the adjacent powder particles. In this study, sintering process is done with heat treatment furnace machine (figure 3.4.4.1). Based on the parameters of sintering, these firing process is based on single ramp-up sintering temperature profile. Every four sample from ratio sample batch 0,3,5,10wt% been heated at 1150, 1200 and 1250°C. Heat treatment furnace machine temperature raised up to sintering profile temperature that already set up (1150,1200 and 1250°C) with heating rate of 5°C/min. The compact ceramic will dwell in this temperature for 3 hours in order to burn all mixture composition. After done heating with profile sintering temperature, the compact porous ceramic will be cooled down in the heat treatment furnace with room temperature at 27 to 28°C. The state of compact porous ceramic after sintering, the porous ceramic should be reach the densified ceramic.

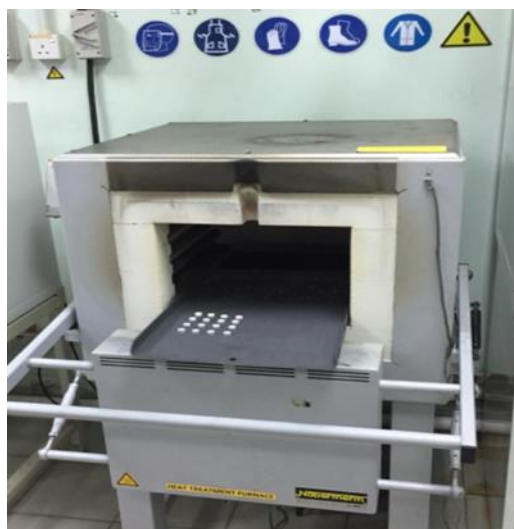


Figure 3.20: Heat Treatment Furnace machine



Figure 3.21: Densified Porous Ceramic samples

3.5 Testing of Powder and Ceramic

The performance of porous ceramic materials is always evaluated in terms of their porosity, density, and mechanical qualities such as hardness. The characteristics of porous ceramic are investigated in this study using nano-carbon black at concentrations of 0%, 3%, 5%, and 10%.

3.5.1 Density and Porosity (Archimedes Principle)

According to Archimedes' Principle, the buoyant force exerted by a submerged item is equal to the weight of the fluid displaced by the object. The apparent porosity and density can be measured using the Archimedes buoyancy technique with W_a is the dry mass, W_c is the saturated mass and W_b is mass suspended in water.

After heating, the dry mass (W_a) of specimens was measured by a precision balance A&D FZ-300i-EC with accuracy of 0.0001g. The specimens were stored in distilled water for a few minutes. After impregnation the saturated mass (W_c) and mass suspended in water (W_b) were measured using the same scale. The collected data were analyzed to apply for the apparent porosity and density formula.



Figure 3.22: A&D FZ-300i-EC Precision Balance



Figure 3.23: Laboratory Archimedes setup

3.5.2 Rockwell Hardness Test

The term "hardness" refers to a material's resistance to plastic deformation caused by indentation. Occasionally, the term "hardness" refers to a material's resistance to

scratching or abrasion. In some circumstances, a reasonably rapid and straightforward hardness test may be used in place of the tensile test. Hardness can be determined without damaging a small sample of material. There are hardness methods that enable on-site hardness measurement.

Any hardness test method is based on the principle of pressing an indenter into the sample surface and then measuring the dimensions of the indentation depth or the indentation's actual surface area. The chemical composition and microstructure features of ceramics determine their hardness: porosity, grain size, and grain-boundary phases.

The Rockwell test is used to determine the depth of penetration of the indenter into the specimen surface. The hardness test is measured with Mitutoyo HR-400 hardness tester and the indenter used is a spheroconical diamond ball. The loading technique begins with the application of a preliminary test force of 10kgf, followed by zeroing out the indicator that measures penetration depth. Following that, a large load of 60 kgf is applied. The penetration depth is determined after the principal load has been removed. Hardness is quantified using “A” scales and numerical values, with no units.



Figure 3.24: Mitutoyo HR-400 Hardness Tester



Figure 3.25: Diamond Ball Indenter

3.5.3 XRD Test

XRD analysis, which involves the study of the crystal structure of a substance, is used to determine the crystalline phases contained in a material and, as a result, to reveal information about its chemical composition. By comparing the data collected to that included in reference databases, it is possible to determine the phases of the process.

X-ray diffraction is a useful technique for determining the composition of minerals, polymers, corrosion products, and other unknown materials, among other things. Element evaluates the vast majority of materials by the use of powder diffraction on finely powdered particles at its testing facility.

This test method involves shining an x-ray beam onto a sample and measuring the scattered intensity as a function of the direction from which the beam was emitted. Once the beam has been separated, the scattering pattern, also known as a diffraction pattern, can be seen, which reveals the crystalline structure of the substance being analysed in the experiment. Next, the Rietveld refinement approach is used to determine the crystal structure that is most likely responsible for the pattern that has been discovered so far.

3.5.4 Scanning Electron Microscope (SEM)

Scanning electron microscopy (SEM) is a sophisticated technique for capturing images of the microstructures of materials. SEM is normally carried out in a vacuum environment due to the tendency of gas molecules to disrupt the electron beam and the secondary and backscattered electrons used for imaging. To characterise the specimens in this research, the microstructure picture was captured using a ZEISS EVO 18.

Dry and clean samples are required before scanning. Mounting the sample was done with an adhesive tab attached to the aluminium stub. Ensure the vacuum chamber is ventilated by running the vent process. Place the specimen in the sample holder and shut the room door when you're done. Afterwards, keep running the pump until it reaches its maximum level of vacuum. The sample is now ready for testing.

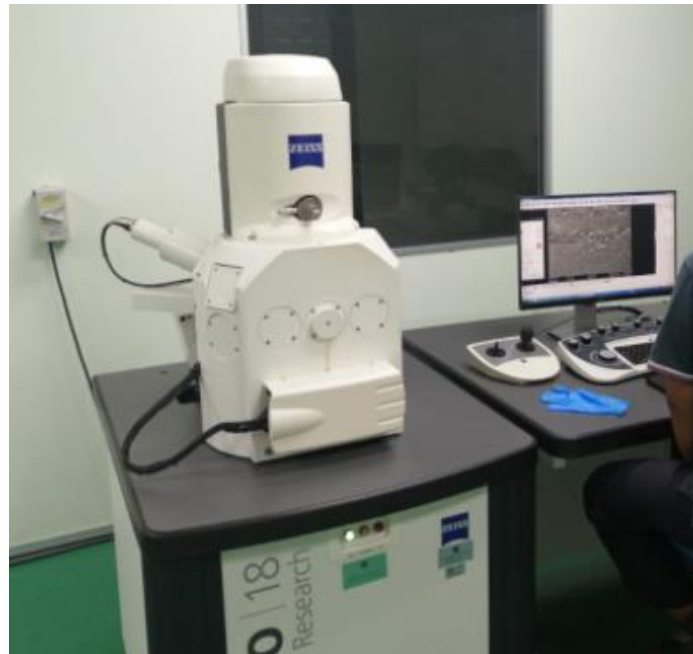


Figure 3.26: ZEISS EVO 18 model



CHAPTER 4

RESULTS AND DISCUSSION

4.1 Introduction

This chapter consists the result of Rockwell Hardness test, Scanning Electron Microscopy (SEM) and Microstructure Microscope analysis test will be shown. The Rockwell hardness test was tested by Mitutoyo HR-400 hardness tester, Porosity/Density test was conducted by using Archimedes's principle and XRD analysis was performed by

4.2 Rockwell Hardness Test

The hardness of the specimens was measured by Mitutoyo HR-400 hardness tester. 3 reading was taken for each porous ceramic sample, 0wt%, 3wt%, 5wt% and 10wt% and different temperature of sintering, 1150°C and 1200 °C. The average value was calculated and comparison for the hardness of each porous ceramic sample will be shown.

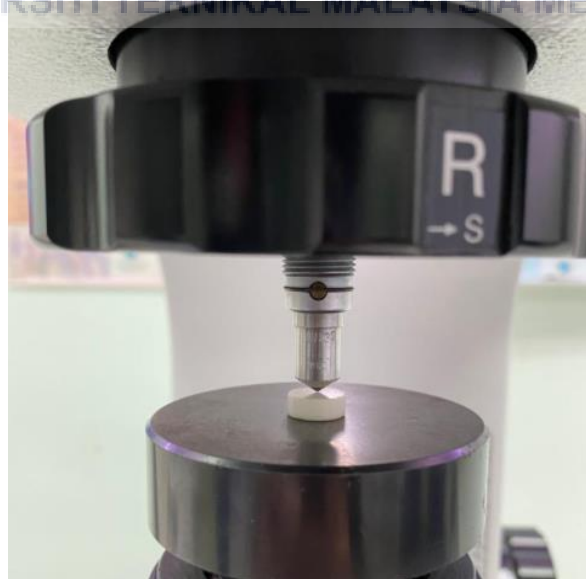


Figure 4.1: Hardness Test

Table 4.1: Result for Rockwell Hardness Test

Sample	1150°C					1200°C				
	1	2	3	Avg	SD	1	2	3	Avg	SD
0wt%	58.8	53.4	76.4	62.87	9.82	53.3	43.0	42.1	46.13	5.08
3wt%	78.5	76.9	54.9	70.1	10.77	52.4	76.7	64.0	64.37	9.92
5wt%	72.6	46.9	54.3	57.93	10.80	45	65.9	66.9	59.27	10.10
10wt%	50.81	51.0	70.4	57.4	9.19	55.1	43.6	51.6	50.1	4.81

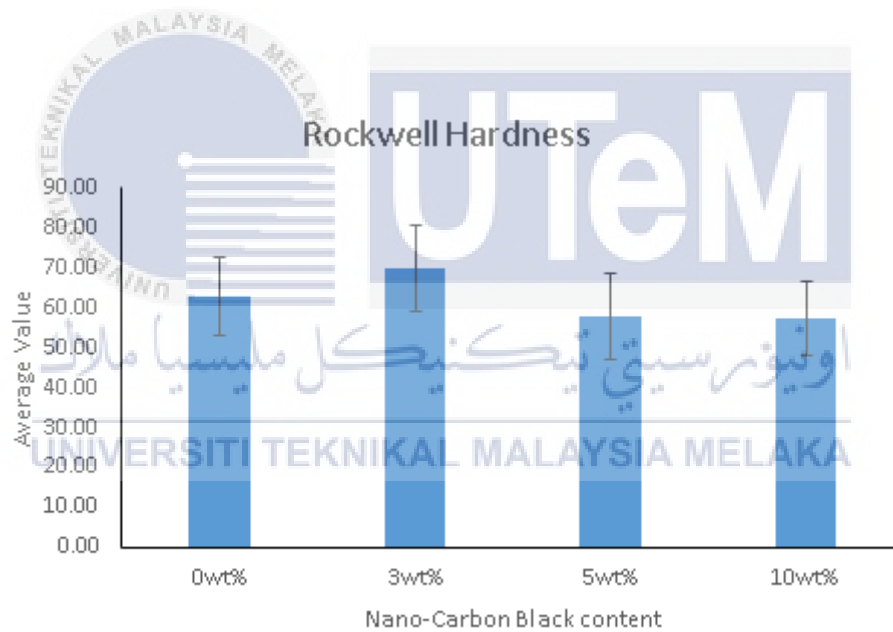


Figure 4.2: Result of Rockwell Hardness Test for 1150°C

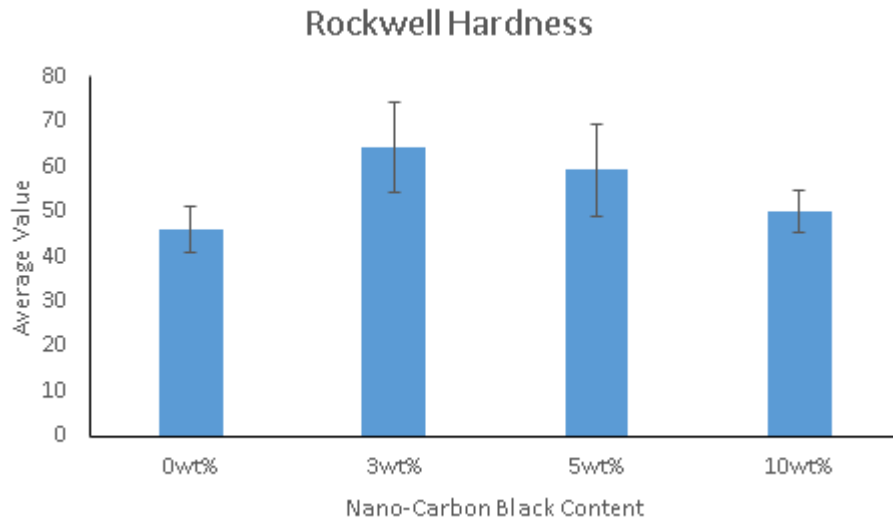


Figure 4.3: Result of Rockwell Hardness Test for 1200°C

The values of the Rockwell Hardness test for each batch, as well as their average and standard values, are shown in Table 4.1 and Figure 4.2-4.3. As illustrated in Figure 4.2, the result for 1150°C samples with a 10wt percent nano-carbon black concentration has the lowest Rockwell Hardness value of 57.4 HRA. We can deduce from this value that the structure is less sturdy due to the absence of nano-carbon black in the composite. The maximum rockwell hardness rating is 70.1 HRA at 3wt%. It can be discovered that the greater the amount of nano-carbon black in the sample, the more delicate it is. The result for 0wt% likewise indicates that the sample has a high hardness value, albeit slightly lower than the figure for 3wt percent nano-carbon black content, which is 62.87 HRA for 0wt% percent.

Meanwhile, as illustrated in Figure 4.3, the result for 1200°C samples demonstrates that 3wt percent nano-carbon black content has the maximum Rockwell Hardness value of 64.37 HRA. This result indicates that the construction is more sturdy due to the addition of nano-carbon black to the composite. However, the lowest number is 46.13 HRA from

0wt%. When significant weights are applied in a hardness test, cracking and spalling create issues. They can make reading the indentation size difficult in some circumstances. Furthermore, because hardness is inversely proportional to the square of the indentation's diagonal length, any measurement inaccuracy is doubled. The result for 0wt% indicates the probability of cracking or spalling occurring on the sample's surface during the hardness test. Furthermore, the result from 10wt% indicates that the sample has a low hardness value after 0wt percent, which is 50.1wt%.

According to table 4.1, figures 4.2 and 4.3, the standard deviation values for all nano-carbon black content samples at 1150°C and 1200°C were greater. Throughout the trials, values varied significantly, for example, sample temperature 1150°C 10%, the first and second trials' values were not significantly different at 50.81HRA and 51.0HRA, respectively, but the third trial's value soared to 70.4HRA. Due to the variability in results between trials, the standard deviation values are large. All samples exhibit a large standard deviation for this hardness test due to the non-uniform microstructure of porous ceramics. With regards to the "Rockwell hardness" test, it has a disadvantage throughout the experimental procedure because estimating the circular angle shape and length of indents involves a certain amount of error that is depending on the load level. These variables may contribute to an increase in the standard deviation of hardness measured with the Rockwell indenter.

4.3 Porosity/Density (Archimedes Principle)

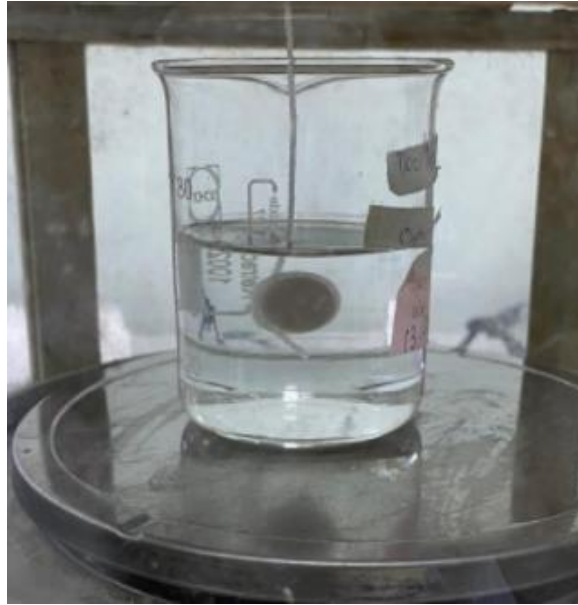


Figure 4.4: Archimedes Principle

Archimedes' principle was used to determine the porosity/density of the samples. The apparent porosity was calculated using Archimedes's principle according to the following formula:

$$P = \frac{W_c - W_a}{W_c - W_b} \times 100$$

Where, P is the apparent porosity, W_a is the dry mass, W_c is the saturated mass and W_b is mass suspended in water.

Each sample of nano-carbon black with a concentration of 0wt%, 3wt%, 5wt%, and 10wt% was analysed twice for W_a , W_b , and W_c . The result was then multiplied by Archimedes' principal formula to obtain the apparent porosity of each sample.

Table 4.2: Result of Apparent Porosity for 1150°C

Sample	Wa (g)	Wb (g)	Wc (g)	Apparent Porosity (%)	Average Apparent Porosity (%)	Standard Deviation
0wt%	0.716	0.298	0.718	0.48	0.45	0.03
	0.929	0.457	0.931	0.42		
3wt%	0.917	0.397	0.919	0.38	0.51	0.13
	0.846	0.373	0.849	0.63		
5wt%	0.797	0.345	0.800	0.66	0.77	0.11
	0.792	0.344	0.796	0.88		
10wt%	0.975	0.426	0.982	1.26	1.67	0.41
	0.927	0.407	0.938	2.07		

UNIVERSITI TEKNIKAL MALAYSIA MELAKA

Table 4.3: Result of Apparent Porosity for 1200°C

Sample	Wa (g)	Wb (g)	Wc (g)	Apparent Porosity (%)	Average Apparent Porosity (%)	Standard Deviation
0wt%	0.893	0.395	0.896	0.59	0.56	0.03
	0.996	0.435	0.999	0.53		
3wt%	0.983	0.455	0.986	0.56	0.62	0.06
	1.060	0.473	1.064	0.67		
5wt%	0.816	0.368	0.822	1.32	1.08	0.24
	0.844	0.373	0.848	0.84		
10wt%	0.998	0.442	1.007	1.59	1.88	0.29
	0.823	0.371	0.833	2.16		

UNIVERSITI TEKNIKAL MALAYSIA MELAKA

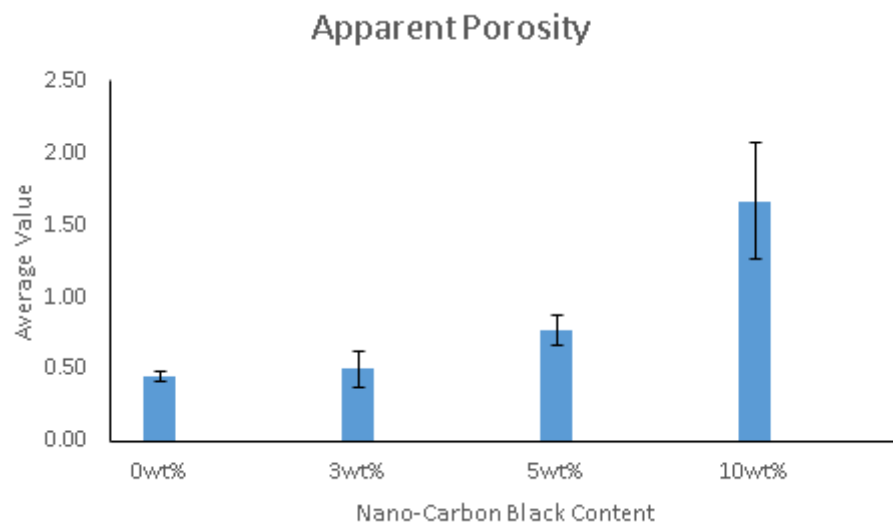


Figure 4.5: Result of Apparent Porosity for 1150°C

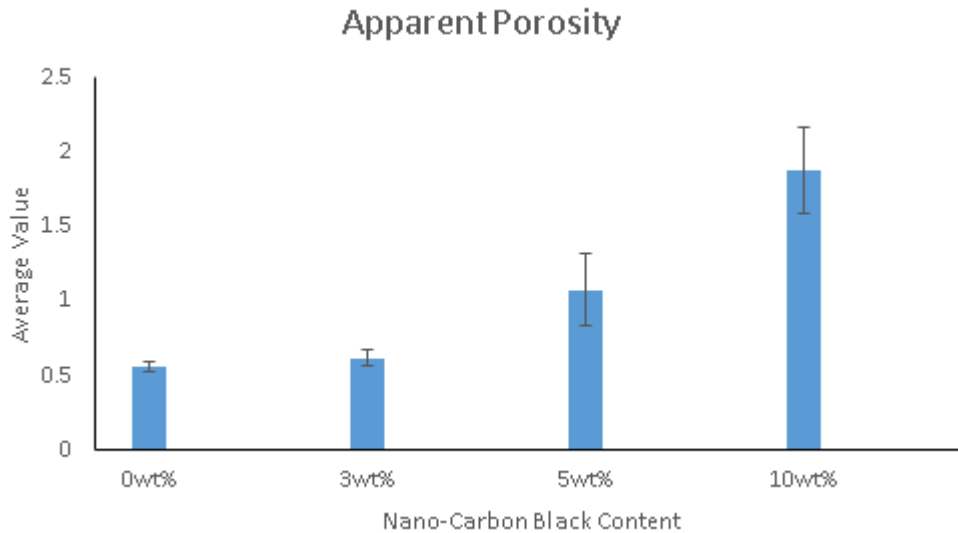


Figure 4.6: Result of Apparent Porosity for 1200°C

The values of average apparent porosity and standard deviation for each batch at 1150°C and 1200°C are shown in Table 4.2-4.3 and Figure 4.5-4.6. Referring to Table 4.2, which summarizes all of the average values, the result indicates that a 0wt% nano-carbon black concentration has the lowest apparent porosity of 0.45%. It may be inferred from this result that the less nano-carbon black is used, the lower the apparent porosity in the ceramics. Meanwhile, 10wt% has the maximum amount which is 1.67%. It is possible to ascertain that the higher the content of nano-carbon black, the greater the apparent porosity. To support this point, reference can be made to Figure 4.5, which shows that when the concentration of nano-carbon black increases, the average apparent porosity also increases. The graph is directly proportionate to the rise.

Additionally, referring to Table 4.3, which summarises all the average values for 1200°C, the results indicate that 10% nano-carbon black content has the maximum apparent porosity value of 1.88%. This value confirms the previous result: the more nano-carbon black used, the greater the apparent porosity in the composite. Additionally, 0wt%

has the lowest value which is 0.56%. It is possible to ascertain that the lower the content of nano-carbon black, the lower the apparent porosity. According to Figure 4.6, the graph indicates that the graph increases directly proportional to the amount of nano-carbon black used in the composite, implying that the amount of nano-carbon black used in the composite is one of the factors contributing to the apparent porosity observed in the samples.

4.4 Scanning Electron Microscope

To characterize the specimens in this analysis, the microstructure picture was captured using a ZEISS EVO 18. Analyses were performed with both secondary and backscattered electron detectors, with 15kV acceleration voltage and working distance of about 8.0 mm. The microstructure image was shown in Figure 4.7 and Figure 4.8.

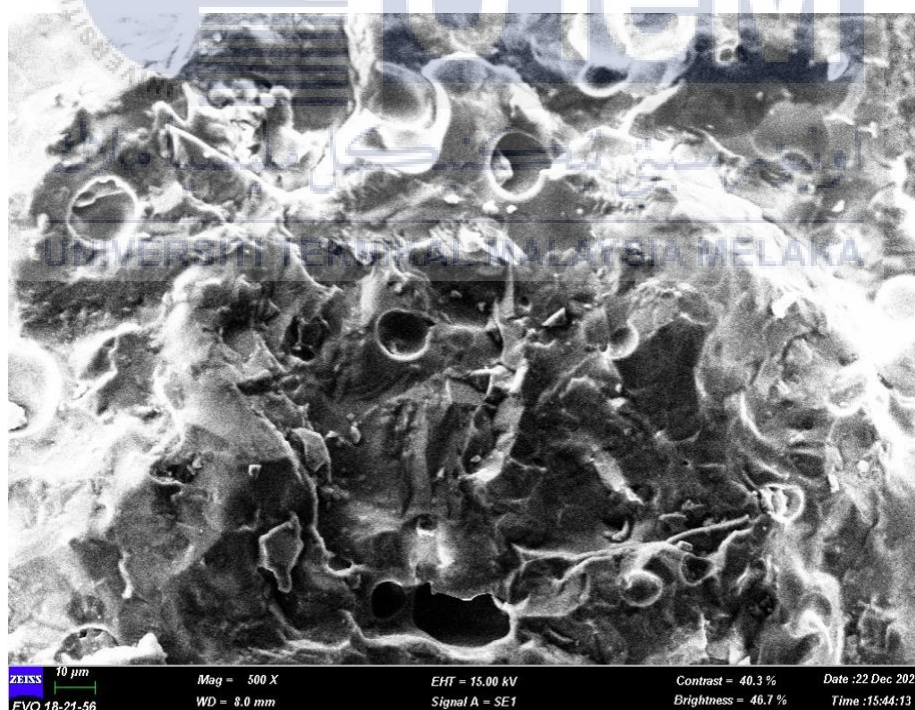


Figure 4.7: SEM characterization of sintered discs produced with nano-carbon black as pore forming agent

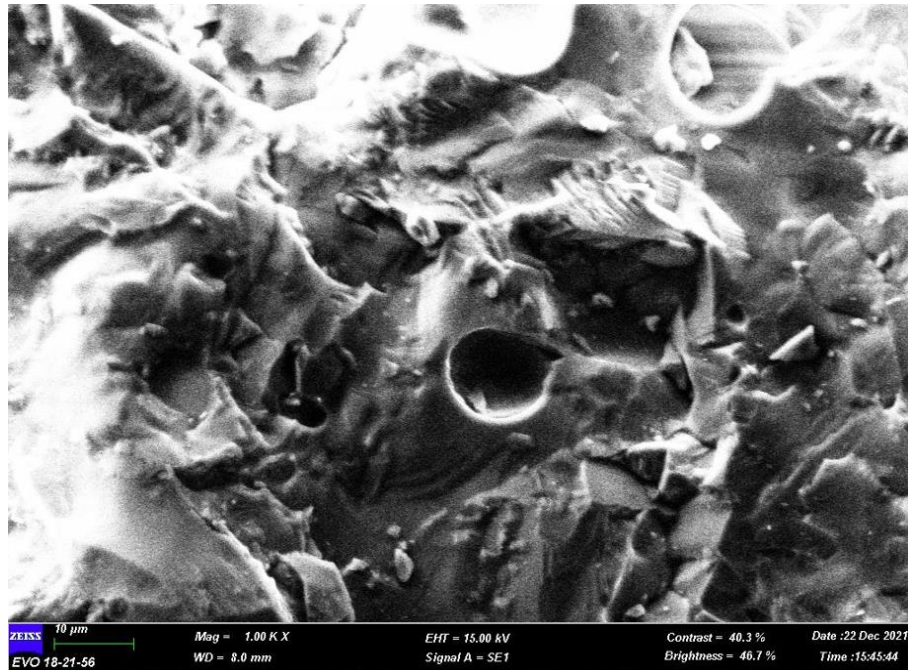


Figure 4.8: SEM characterization of sintered discs produced with nano-carbon black as pore forming agent

Referring to the figure 4.7 and 4.8 present SEM micrographs of the prepared porous ceramics. The SEM micrographs correspond to the porous cross sectional area of each samples.



4.5 X-Ray Diffraction analysis

Analysis of ceramic structure and phase was carried out by XRD. The XRD pattern of porous ceramics prepared without nano-carbon black is shown in Figure 4.7. As seen, the XRD pattern of basic ceramics such as $\text{Al}_2\text{O}_3 \cdot 2\text{SiO}_2 \cdot 2\text{H}_2\text{O}$ (kaolinite), SiO_2 (silica) and KAlSi_3O_8 (feldspar) were clearly detected. This indicates that the main structure and phase of ceramics were successfully produced after sintering. However, there were also found that the presence of unknown phase with small peaks. It is believed that the unknown phase could be the intermediate phase of the respective ceramic content.

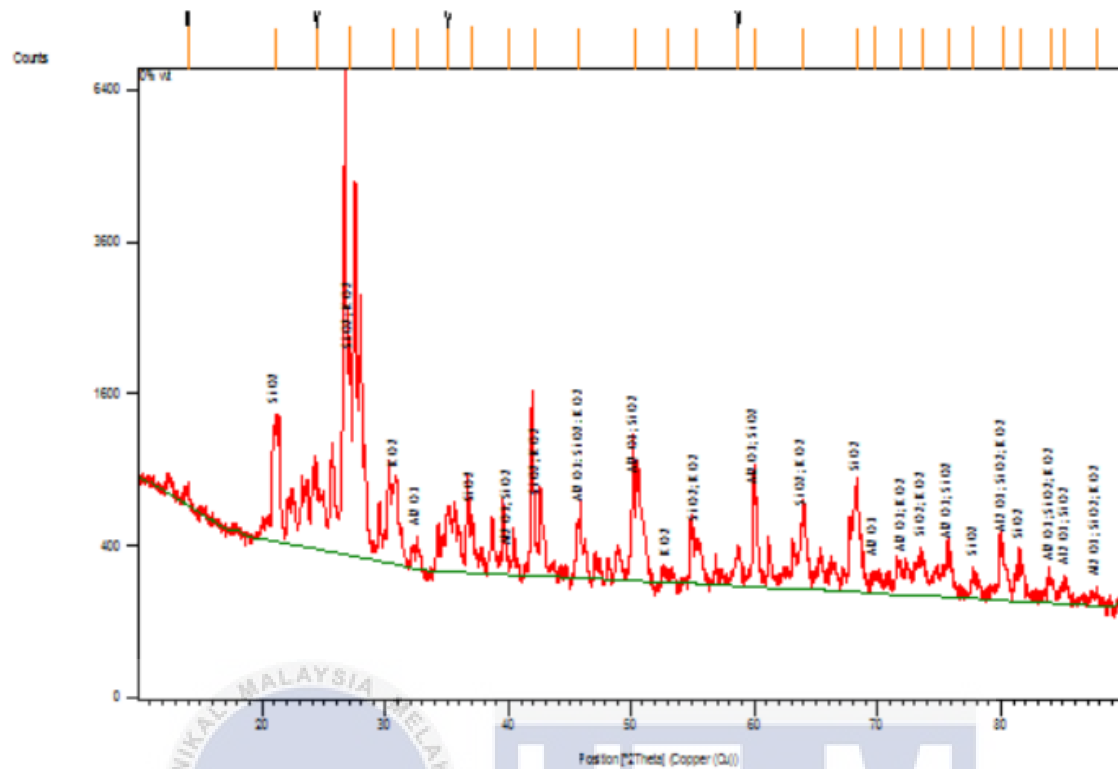


Figure 4.9: Porous ceramic diffraction pattern on 0wt% nano carbon black content

CHAPTER 5

CONCLUSION AND RECOMMENDATION

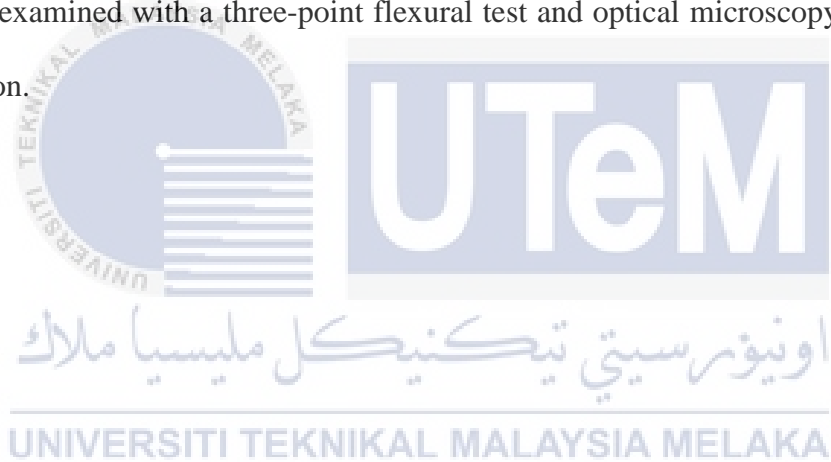
5.1 Conclusion

This chapter concluded the study of the experiment's outcomes and findings. This chapter concludes with a number of recommendations and findings. This research is primarily focused on the development of porosity in ceramic composites for the preparation and fabrication of porous ceramics. Additionally, the mechanical properties of porous ceramics were determined using the Rockwell hardness test. Each sample contains 0wt%, 3wt%, 5wt%, and 10% nano-carbon black.

The findings indicate that increasing the porous ceramic of nano-carbon black composite by 3wt% to 10wt% increases apparent porosity and density. The percentage of porosity in the porous ceramic was proportional to the amount of pore forming agent used; the more the percentage of pore forming agent used in, the greater the percentage of porosity in the porous ceramic. However, by incorporating porosity into porous ceramics, heat conductivity is reduced while the mechanical resistance of the porous ceramics is decreased. As a result of this analysis, it was determined that the larger the percentage of pore forming agent used, the lower the hardness values of the porous ceramic. However, the created porous ceramics retain an acceptable level of mechanical strength which is the lowest value for hardness is 46.13HRA.

5.2 Recommendation

The work can be expanded to evaluate additional properties of the composite by altering the type of pore forming agent, the volume weight of the composite mixture, the percentage weight of nano-carbon black, and the shape and size of the porous ceramic sample. The technique of fabricating porous ceramic compositions should be tuned, including the pressure used during the compression process and the sintering parameter used during the heat treatment. This can improve the composite's mechanical qualities, and additional porosity and density tests should be conducted to assess the composite's mechanical properties. Rather than performing a Rockwell hardness test, the specimen should be examined with a three-point flexural test and optical microscopy for extensive examination.



REFERENCES

- Adler, J. (2005). Ceramic diesel particulate filters. *International Journal of Applied Ceramic Technology*, 2(6), 429–439. <https://doi.org/10.1111/j.1744-7402.2005.02044.x>
- Brindley, G. W., Editors, B. G., & Structures, C. (1981). *Reviews*. 1981.
- Bockhorn, H., Hornung, A., Hornung, U., & Schawaller, D. (1999). Kinetic study on the thermal degradation of polypropylene and polyethylene. *Journal of Analytical and Applied Pyrolysis*, 48(2), 93–109. [https://doi.org/10.1016/S0165-2370\(98\)00131-4](https://doi.org/10.1016/S0165-2370(98)00131-4)
- Carneiro, J., Tobaldi, D. M., Capela, M. N., Novais, R. M., Seabra, M. P., & Labrincha, J. A. (2018). Synthesis of ceramic pigments from industrial wastes: Red mud and electroplating sludge. *Waste Management*, 80, 371–378. <https://doi.org/10.1016/j.wasman.2018.09.032>
- Dai, J., Xu, X. L., Yang, J. H., Zhang, N., Huang, T., Wang, Y., Zhou, Z. W., & Zhang, C. L. (2015). Greatly enhanced porosity of stretched polypropylene/graphene oxide composite membrane achieved by adding pore-forming agent. *RSC Advances*, 5(27), 20663–20673. <https://doi.org/10.1039/c4ra13298j>
- Do, T., Shin, C., Kwon, P., & Yeom, J. (2016). Fully-enclosed ceramic micro-burners using fugitive phase and powder-based processing. *Scientific Reports*, 6(August), 1–12. <https://doi.org/10.1038/srep31336>
- Eb, C. (2019). *Investigation of the Thermal Conductivity and the Viscosity of Carbon Black Heat Transfer Nanofluids*. June, 26–28.
- Effting, C., Güths, S., & Alarcon, O. E. (2007). Evaluation of the thermal comfort of ceramic floor tiles. *Materials Research*, 10(3), 301–307. <https://doi.org/10.1590/s1516-14392007000300016>
- Elias, M. B., Machado, R., & Canevarolo, S. V. (2000). Thermal and dynamic-mechanical characterization of uni- and biaxially oriented polypropylene films. *Journal of Thermal Analysis and Calorimetry*, 59(1), 143–155. <https://doi.org/10.1023/A:1010187913049>
- Gaydardzhiev, S., Gusovius, H., Wilker, V., & Ay, P. (2008). Gel-casted porous Al₂O₃ ceramics by use of natural fibres as pore developers. *Journal of Porous Materials*, 15(4), 475–480. <https://doi.org/10.1007/s10934-007-9099-1>
- German, R. M., Suri, P., & Park, S. J. (2009). Review: Liquid phase sintering. *Journal of Materials Science*, 44(1), 1–39. <https://doi.org/10.1007/s10853-008-3008-0>
- Gregorová, E., & Pabst, W. (2011). Process control and optimized preparation of porous alumina ceramics by starch consolidation casting. *Journal of the European*

Ceramic Society, 31(12), 2073–2081.
<https://doi.org/10.1016/j.jeurceramsoc.2011.05.018>

Gregorová, E., & Pabst, W. (2007). Porous ceramics prepared using poppy seed as a pore-forming agent. *Ceramics International*, 33(7), 1385–1388.
<https://doi.org/10.1016/j.ceramint.2006.05.019>

Hisham A. Maddah. (2016). Polypropylene as a Promising Plastic: A Review. *American Journal of Polymer Science*. <https://doi.org/10.5923/j.ajps.20160601.01>

Hong, L., Wang, Z., Wang, S., & Xu, M. (2018). Preparation of Silicon Carbide porous Ceramics. *IOP Conference Series: Materials Science and Engineering*, 394(2).
<https://doi.org/10.1088/1757-899X/394/2/022070>

Lerari, D., Peeterbroeck, S., Benali, S., Benaboura, A., & Dubois, P. (2010). Use of a new natural clay to produce poly(methylmethacrylate)-based nanocomposites. *Polymer International*, 59(1), 71–77. <https://doi.org/10.1002/pi.2691>

Liu, J., Li, Y., Li, Y., Sang, S., & Li, S. (2016). Effects of pore structure on thermal conductivity and strength of alumina porous ceramics using carbon black as pore-forming agent. *Ceramics International*, 42(7), 8221–8228.
<https://doi.org/10.1016/j.ceramint.2016.02.032>

Matsuyama, H., Maki, T., Teramoto, M., & Asano, K. (2002). Effect of polypropylene molecular weight on porous membrane formation by thermally induced phase separation. *Journal of Membrane Science*, 204(1–2), 323–328.
[https://doi.org/10.1016/S0376-7388\(02\)00056-X](https://doi.org/10.1016/S0376-7388(02)00056-X)

Mattern, A., Huchler, B., Staudenecker, D., Oberacker, R., Nagel, A., & Hoffmann, M. J. (2004). Preparation of interpenetrating ceramic-metal composites. *Journal of the European Ceramic Society*, 24(12), 3399–3408.
<https://doi.org/10.1016/j.jeurceramsoc.2003.10.030>

Meneghetti, P., & Qutubuddin, S. (2006). Synthesis, thermal properties and applications of polymer-clay nanocomposites. *Thermochimica Acta*, 442(1–2), 74–77.
<https://doi.org/10.1016/j.tca.2006.01.017>

Misyura, S. Y. (2016). The influence of porosity and structural parameters on different kinds of gas hydrate dissociation. *Scientific Reports*, 6(July), 1–10.
<https://doi.org/10.1038/srep30324>

Mylona, S. (n.d.). *Investigation of the Thermal Conductivity and the Viscosity of Carbon Black Heat Transfer Nanofluids*.

Nimmo, J. R. (2013). Porosity and Pore Size Distribution. In *Reference Module in Earth Systems and Environmental Sciences*. Published by Elsevier Inc.
<https://doi.org/10.1016/b978-0-12-409548-9.05265-9>

Novais, R. M., Seabra, M. P., & Labrincha, J. A. (2014). Ceramic tiles with controlled porosity and low thermal conductivity by using pore-forming agents. *Ceramics International*, 40(8 PART A), 11637–11648. <https://doi.org/10.1016/j.ceramint.2014.03.163>

Novais, R. M., Seabra, M. P., & Labrincha, J. A. (2014). Ceramic tiles with controlled porosity and low thermal conductivity by using pore-forming agents. *Ceramics International*, 40(8 PART A), 11637–11648. <https://doi.org/10.1016/j.ceramint.2014.03.163>

P. E. Khizhnyak, A. V. Chechetkin, A. A. . . G. (1980). *T a b l e 4*. 37(3), 1073–1075.

Resources, R. C. (2017). *F09 SI: THERMAL COMFORT. 1*.

Rice, R. W. (1996). Grain size and porosity dependence of ceramic fracture energy and toughness at 22°C. *Journal of Materials Science*, 31(8), 1969–1983. <https://doi.org/10.1007/BF00356616>

Sadeghi, F., Ajji, A., & Carreau, P. J. (2007). Analysis of microporous membranes obtained from polypropylene films by stretching. *Journal of Membrane Science*, 292(1–2), 62–71. <https://doi.org/10.1016/j.memsci.2007.01.023>

Sahoo, P. K., & Samal, R. (2007). Fire retardancy and biodegradability of poly(methyl methacrylate)/montmorillonite nanocomposite. *Polymer Degradation and Stability*, 92(9), 1700–1707. <https://doi.org/10.1016/j.polymdegradstab.2007.06.003>

Science, M. (1975). 20 (1975) 89--93 © Elsevier Sequoia S.A., Lausanne --Printed in The Netherlands Porosity--Thermal Conductivity Correlations for Ceramic Materials. 20, 89–93.

Wilder, G. J. (1970). Structure of Tracheids in Three Species of Lycopodium. *American Journal of Botany*, 57(9), 1093–1107. <https://doi.org/10.1002/j.1537-2197.1970.tb09913.x>

Živcová, Z., Gregorová, E., & Pabst, W. (2007). Porous alumina ceramics produced with lycopodium spores as pore-forming agents. *Journal of Materials Science*, 42(20), 8760–8764. <https://doi.org/10.1007/s10853-007-1852-y>



اونيورسيتي تيكنيكل مليسيا ملاك

UNIVERSITI TEKNIKAL MALAYSIA MELAKA

APPENDICES

APPENDIX A: GANTT CHART PSM 1

NO	TASK PROJECT	PLAN/ ACTUAL	WEEK														
			1	2	3	4	5	6	7	8	9	10	11	12	13	14	15
1	Supervisor selection and registered title.	Plan															
		Actual															
2	Brief and project explanation by supervisor.	Plan									M						
		Actual									I						
3	Drafting Literature Review and writing up Chapter 2.	Plan									D						
		Actual									T						
4	Submission Drafting of Chapter 2.	Plan									E						
		Actual									R						
5	Discuss on methodology with supervisor	Plan									M						
		Actual															
6	Research on methodology and writing up Chapter 3.	Plan									B						
		Actual									R						
7	Discuss and writing problem statement and objective for	Plan									E						
		Actual									A						
8	Writing up Preliminary Result.	Plan									K						
		Actual															
9	Submission of first draft PSM 1.	Plan															
		Actual															
10	Preparation and presentation PSM 1.	Plan															
		Actual															

APPENDIX B: GANTT CHART PSM 2

NO	TASK PROJECT	PLAN/ ACTUAL	WEEK														
			1	2	3	4	5	6	7	8	9	10	11	12	13	14	15
1	Meeting and discussion.	Plan															
		Actual															
2	Determine the chemical equation and parameter for	Plan															
		Actual															
3	Prepare and mixing sample composition for 0wt% and 3wt%	Plan															
		Actual															
4	Prepare and mixing sample composition for 5wt% and 10wt%	Plan															
		Actual															
5	Sieving process	Plan															
		Actual															
6	Compress process	Plan															
		Actual															
7	Sintering process	Plan															
		Actual															
8	Do Hardness, XRD and Archimedes test.	Plan															
		Actual															
9	Preparation and presentation FYP 2.	Plan															
		Actual															

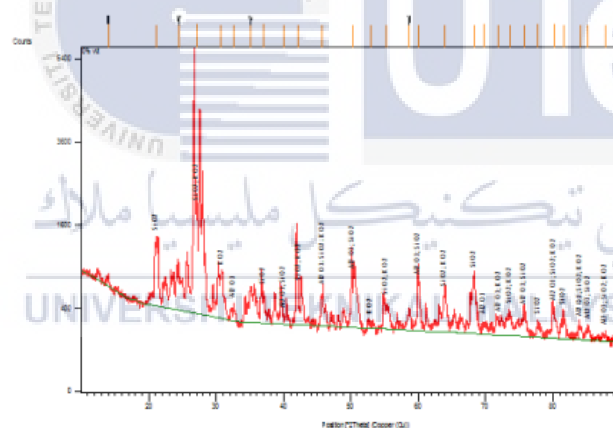
APPENDIX C: XRD Result 0wt% Nano-carbon black

Date: 5/1/2022 Time: 3:45:05 PM File: 0% wt User: MAKMAL FIZIK 2-1

Anchor Scan Parameters

Dataset Name: 0% wt
 File name: C:\Users\MAKMAL FIZIK 2-1\Desktop\bookin\XRD-05012022\0% wt.xrdml
 Comment: Configuration=Stage Flat Sample, Owner=User-1, Creation date=5/10/2007 1:44:12 PM
 Goniometer=Pw3050/60 (Theta/Theta); Minimum step size 2Theta:0.001; Minimum step size Omega:0.001
 Sample stage=Pw3071/xx Bracket
 Diffractometer system=PERT-PRO
 Measurement program=Test 30 to 60 deg FlatStage, Owner=User-1, Creation date=1/8/2008 9:47:53 AM
 Measurement Date / Time: 5/1/2022 3:03:07 PM
 Operator: Administrator
 Raw Data Origin: XRD measurement (*.XRDML)
 Scan Axis: Goni
 Start Position [2Th.]: 10.0114
 End Position [2Th.]: 89.9794
 Step Size [2Th.]: 0.0170
 Scan Step Time [s]: 43.2865
 Scan Type: Continuous
 PSD Mode: Scanning
 PSD Length [2Th.]: 2.12
 Offset [2Th.]: 0.0000
 Divergence Slit Type: Fixed
 Divergence Slit Size [°]: 0.5000
 Specimen Length [mm]: 10.00
 Measurement Temperature [°C]: 25.00
 Anode Material: Cu
 K-Alpha1 [Å]: 1.54060
 K-Alpha2 [Å]: 1.54443
 K-Beta [Å]: 1.39225
 K-A2 / K-A1 Ratio: 0.50000
 Generator Settings: 30 mA, 40 kV
 Diffractometer Type: 0000000011024214
 Diffractometer Number: 0
 Goniometer Radius [mm]: 240.00
 Dist. Focus-Diverg. Slit [mm]: 100.00
 Incident Beam Monochromator: No
 Spinning: No

Graphics



1 Of 4

Peak List

Pos. [°2Th.]	Height [cts]	FWHM [°2Th.]	d-spacing [Å]	Rel. Int. [%]
13.9669	109.07	0.5353	6.34086	7.04
21.1633	895.75	0.5353	4.19816	57.84
24.4040	439.76	1.0706	3.64753	28.40
27.0229	1548.54	1.0706	3.29969	100.00
30.6713	470.55	0.8029	2.91499	30.39
32.5841	118.13	0.6691	2.74811	7.63
35.0320	345.13	0.5353	2.56149	22.29
36.9085	273.77	0.5353	2.43546	17.68
39.9269	46.09	1.0706	2.25803	2.98
42.1363	337.64	0.8029	2.14460	21.80
45.7017	300.49	0.5353	1.98524	19.41
50.3527	503.44	0.6691	1.81224	32.51
53.0195	32.75	0.5353	1.72720	2.11
55.2857	210.49	0.8029	1.66165	13.59
58.7031	167.33	0.5353	1.57280	10.81
60.0837	438.29	0.5353	1.53993	28.30
63.9306	322.89	0.8029	1.45623	20.85
68.3379	550.42	0.6691	1.37267	35.54
69.7232	72.81	0.6691	1.34875	4.70
71.9831	97.47	0.8029	1.31186	6.29
73.6068	171.82	0.5353	1.28689	11.10
75.7657	165.45	0.8029	1.25550	10.68
77.8005	93.99	0.5353	1.22767	6.07
80.0903	212.80	0.8029	1.19824	13.74
81.5556	176.13	0.5353	1.18038	11.37
84.0235	89.68	0.5353	1.15189	5.79
85.2014	77.30	0.5353	1.13895	4.99
87.7565	36.12	0.9792	1.11134	2.33

Pattern List

Visible	Ref. Code	Score	Compound Name	Displ. [°2Th]	Scale Fac.	Chem.
Formula						
	00-056-0457	16	α-Al ₂ O ₃	0.000	0.063	Al ₂ O ₃
	00-033-1161	39	silica, low quartz	0.000	0.561	Si O ₂
	00-043-1020	8	Potassium Oxide	0.000	0.100	K O ₂

Document History

Insert Measurement:

- File name = "0% wt.xrdm"
 - Modification time = "5/1/2022 3:39:40 PM"
 - Modification editor = "MAKMAL FIZIK 2-1"

Default properties:

- Measurement step axis = "None"
 - Internal wavelengths used from anode material: Copper (Cu)
 - Original K-Alpha1 wavelength = "1.54060"
 - Used K-Alpha1 wavelength = "1.54060"
 - Original K-Alpha2 wavelength = "1.54443"
 - Used K-Alpha2 wavelength = "1.54443"
 - Original K-Beta wavelength = "1.39225"
 - Used K-Beta wavelength = "1.39225"
 - Incident beam monochromator = "No"
 - Irradiated length = "10.00000"
 - Spinner used = "No"
 - Receiving slit size = "0.10000"
 - Step axis value = "0.00000"
 - Offset = "0.00000"

- Data source = "Peak list"
 - Restriction = "Restriction set"
 - Description = "Default - All ref. patterns possible"
 - All of: elements = "O, K"
 - At least one of: elements = ""
 - None of: elements = "H, He, Li, Be, B, C, N, F, Ne, Na, Mg, Al, Si, P, S, Cl, Ar, Ca, Sc, Ti, V, Cr, Mn, Fe, Co, Ni, Cu, Zn, Ga, Ge, As, Se, Br, Kr, Rb, Sr, Y, Zr, Nb, Mo, Tc, Ru, Rh, Pd, Ag, Cd, In, Sn, Sb, Te, I, Xe, Cs, Ba, La, Ce, Pr, Nd, Pm, Sm, Eu, Gd, Tb, Dy, Ho, Er, Tm, Yb, Lu, Hf, Ta, W, Re, Os, Ir, Pt, Au, Hg, Tl, Pb, Bi, Po, At, Rn, Fr, Ra, Ac, Th, Pa, U, Np, Pu, Am, Cm, Bk, Cf, Es, Fm, Md, No, Lr, D, T"
 - Maximum no. of elements = "2"
 - Skip marked as deleted by ICDD = "No"
 - Skip marked as deleted by a user = "No"
 - Skip non ambient pressure = "No"
 - Skip non ambient temperature = "No"
 - Skip alternate patterns = "No"
 - Quality marks set = ""
 - Subfiles = ""
 - Scoring schema = "Single phase"
 - Auto residue = "Yes"
 - Match intensity = "Yes"
 - Demote unmatched strong = "Yes"
 - Allow pattern shift = "No"
 - Two theta shift = "0"
 - Identity = "No"
 - Modification time = "5/1/2022 3:42:02 PM"
 - Modification editor = "MAKMAL FIZIK 2-1"

APPENDIX D: XRD Result for Aluminium Oxide

Date: 5/1/2022 Time: 3:44:30 PM File: 0% wt User: MAKMAL FIZIK 2-1

Name and formula

Reference code: 00-056-0457
 Common name: γ -Al₂O₃
 PDF index name: Aluminum Oxide
 Empirical formula: Al₂O₃
 Chemical formula: Al₂O₃

Crystallographic parameters

Crystal system: Cubic
 Space group: Fd-3m
 Space group number: 227
 a (Å): 7.9110
 b (Å): 7.9110
 c (Å): 7.9110
 Alpha (°): 90.0000
 Beta (°): 90.0000
 Gamma (°): 90.0000
 Volume of cell (10⁶ pm³): 495.10
 Z: 11.00
 RIR: -

Subfiles and Quality

Subfiles: Inorganic
 Alloy, metal or intermetallic
 Cement and Hydration Product
 Common Phase
 Forensic
 Pharmaceutical
 Superconducting Material
 Excipient
 Star (S)
 Quality: Star (S)

Comments

Sample preparation: Obtained from a one-shot calcination of deuterated boehmite at 873 K in air for 8 hours.
 Unit cell data source: Rietveld or profile fit analysis.

References

Primary reference: Zhou, R.-S., Snyder, R., **47**, 617, (1991)

Peak list

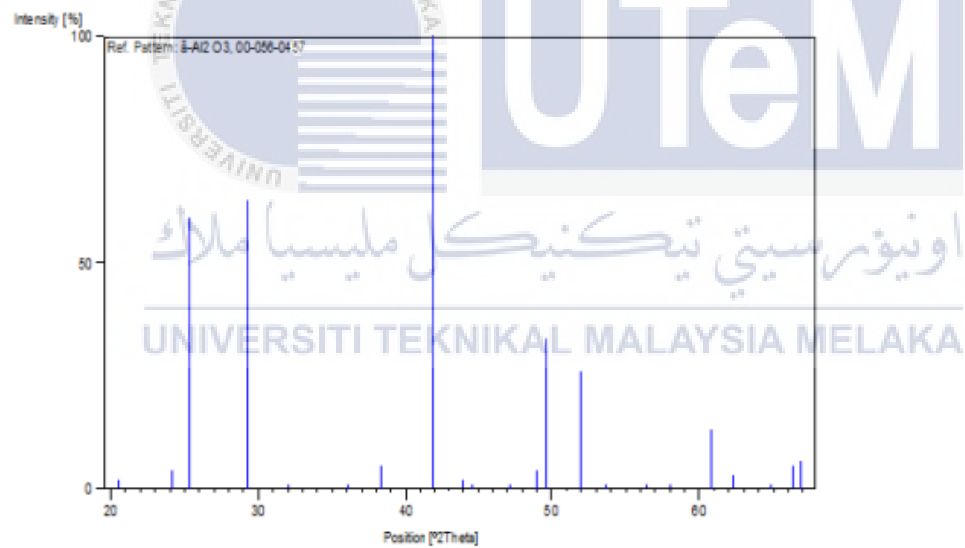
No.	h	k	l	d [Å]	2Theta [deg]	I [%]
1	2	2	0	2.79690	20.596	2.0
2	3	1	1	2.38520	24.201	4.0
3	2	2	2	2.28360	25.295	60.0

Date: 5/1/2022 Time: 3:44:30 PM

File: 0% wt

User: MAKMAL FIZIK 2-1

4	4	0	0	1.97770	29.289	64.0
5	3	3	1	1.81480	31.985	1.0
6	4	2	2	1.61480	36.075	1.0
7	5	1	1	1.52240	38.347	5.0
8	4	4	0	1.39840	41.900	100.0
9	5	3	1	1.33720	43.915	2.0
10	4	4	2	1.31850	44.571	1.0
11	6	2	0	1.25080	47.124	1.0
12	5	3	3	1.20640	48.970	4.0
13	6	2	2	1.19260	49.575	33.0
14	4	4	4	1.14180	51.941	26.0
15	5	5	1	1.10770	53.665	1.0
16	6	4	2	1.05710	56.457	1.0
17	5	5	3	1.02990	58.088	1.0
18	8	0	0	0.98880	60.751	13.0
19	7	3	3	0.96640	62.314	3.0
20	8	2	2	0.93230	64.865	1.0
21	7	5	1	0.91340	66.378	5.0
22	6	6	2	0.90740	66.875	6.0

Stick Pattern

APPENDIX E: XRD Results of Potassium Oxide

Date: 5/1/2022 Time: 3:42:52 PM File: D% ut User: MAHMAL FIZIK 2-1

Name and formula

Reference code: 99-043-1020
 PDF index name: Potassium Oxide
 Empirical formula: KO_2
 Chemical formula: KO_2

Crystallographic parameters

Crystal system: Tetragonal
 Space group: $I4/mmm$
 Space group number: 139

a (Å): 4.0330
 b (Å): 4.0330
 c (Å): 6.6990
 Alpha (°): 90.0000
 Beta (°): 90.0000
 Gamma (°): 90.0000

Calculated density (g/cm³): 2.17
 Volume of cell (10⁻⁶ cm³): 108.96
 Z: 2.00

RIR: 3.04

Subfiles and Quality

Subfiles: Inorganic
 Alloy, metal or intermetallic
 Potassic
 Calculated (C)

Quality:

Comments

General comments: Calculation of diffractometer peak intensities done with MICRO-POWDER 2.2 (D. Smith and K. Smith) using default instrument broadening function (NBS Table), diffracted beam monochromator polarization correction, and atomic scattering factors corrected for anomalous dispersion. Cell parameters from Abrahams, S.
 ANK: See 00-079-0637
 Additional pattern:

References

Primary reference: Grier, D., McCarthy, G., North Dakota State University, Fargo, North Dakota, USA. (1993)

Peak list

h	k	l	h ² +k ² +l ²	d (Å)	2Theta (deg)	I (%)
1	1	0	2	3.95500	16.692	11.0
2	2	0	8	3.34900	17.173	99.0
3	3	0	18	2.85200	20.134	100.0
4	4	0	32	2.41900	26.630	39.0

Date: 5/1/2022 Time: 3:42:52 PM File: D% ut User: MAHMAL FIZIK 2-1

5	2	0	0	2.01600	28.720	20.0
6	1	0	3	1.95350	29.660	21.0
7	2	1	1	1.74160	33.360	3.0
8	2	0	2	1.72760	33.644	15.0
9	0	0	4	1.67470	34.742	1.0
10	1	1	4	1.44410	40.815	1.0
11	2	2	0	1.42890	41.088	6.0
12	2	1	3	1.40310	41.793	11.0
13	3	0	1	1.31810	44.585	1.0
14	2	2	2	1.31200	44.803	5.0
15	2	0	4	1.28940	45.670	1.0
16	3	1	0	1.27530	46.166	8.0
17	1	0	5	1.27150	46.212	10.0
18	3	1	2	1.19190	49.404	6.0
19	3	0	3	1.18170	51.441	2.0
20	0	0	6	1.11650	53.209	1.0
21	3	2	1	1.10330	53.897	1.0
22	2	2	4	1.08570	54.843	1.0
23	2	1	5	1.07550	55.400	7.0
24	1	1	6	1.02970	57.489	1.0
25	3	1	4	1.01460	59.050	1.0
26	4	0	0	1.00820	59.443	1.0
27	3	2	3	1.00010	59.993	3.0
28	2	0	6	0.97480	61.878	1.0
29	4	1	1	0.96790	62.207	1.0
30	4	0	2	0.96550	62.378	2.0
31	3	3	0	0.95060	63.469	1.0
32	3	0	5	0.94900	63.580	3.0
33	1	0	7	0.92110	64.959	2.0
34	3	3	2	0.91450	66.288	1.0
35	4	2	0	0.90180	67.345	2.0
36	4	1	3	0.89800	67.540	2.0

Stick Pattern

APPENDIX F: XRD Results for Silicon Oxide

Date: 5/1/2022 Time: 3:43:56 PM File: 8% wt User: BAA394L PDSH 2-1

Name and formula

Reference code: 00-033-1181
Mineral name: Quartz, 4yt
Common name: silica, low quartz
PDF index name: Silicon Oxide
Empirical formula: SiO_2
Chemical formula: SiO_2

Crystallographic parameters

Crystal system: Hexagonal
Space group: P321
Space group number: 154
a [Å]: 4.0124
b [Å]: 4.0124
c [Å]: 5.4059
Alpha [°]: 90.0000
Beta [°]: 90.0000
Gamma [°]: 120.0000
Calculated density [g/cm³]: 2.65
Measured density [g/cm³]: 2.64
Volume of cell [Å³]: 113.01
Z: 3
PPV: 0.60

Status, subfiles and quality

Status: Alternate Pattern
Subfile: Isomeric
Mineral
Alloy, metal or intermetallic
Cermet and Hydrated Product
Carbide Phase
Educational pattern
Forensic
NIST pattern
Pharmaceutical
Exploit
See [0]

Comments

General comments: Pattern reviewed by Holzer, J., McCarthy, G., North Dakota State Univ., Fargo, North Dakota, USA, ICDD Gas-sil-Ais (1998). Agrees well with experimental and calculated patterns.
Sample source: Sample from the Glass Section at NIST, Gaithersburg, Maryland, USA, ground single-crystals of optical quality.
Additional pattern: See PDF 00-08-1845. See PDF 01-070-1253, 01-089-2146, 01-089-2147, 01-089-2148 and 01-081-8855. To replace 00-089-408 and validated by calculated pattern.

1 of 3

Date: 5/1/2022 Time: 3:43:56 PM File: 8% wt User: BAA394L PDSH 2-1

2θ (deg) 2θ (deg)

Temperature: Pattern taken at 295 K

References

Primary reference: 00-033-1181

Optical data: Search, Phys. 3, 24 (1954)

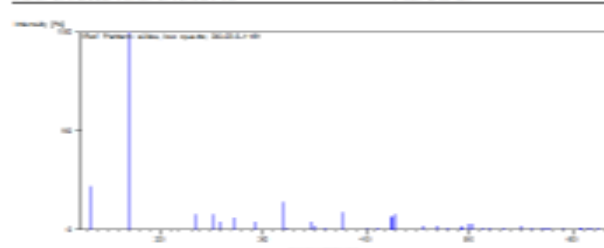
Peak list

h	k	l	h	k	l	2θ (deg)	2θ (deg)	I (a.u.)	I (a.u.)
1	0	0	1	0	0	4.25750	15.499	22.0	
2	0	0	2	0	0	3.24220	17.209	508.0	
3	1	0	3	1	0	2.45140	23.463	8.0	
4	1	0	4	1	0	2.26200	25.513	8.0	
5	1	1	5	1	1	2.23700	26.835	4.0	
6	1	0	6	1	0	2.13700	27.132	4.0	
7	1	0	7	1	0	1.97320	29.264	4.0	
8	1	1	8	1	1	1.91790	31.828	14.0	
9	2	0	9	2	0	1.80210	34.717	8.0	
10	2	0	10	2	0	1.71130	36.902	4.0	
11	2	1	11	2	1	1.63910	39.089	2.0	
12	2	1	12	2	1	1.60540	40.228	1.0	
13	2	1	13	2	1	1.56150	41.544	3.0	
14	2	2	14	2	2	1.53380	43.238	2.0	
15	2	0	15	2	0	1.49380	44.247	1.0	
16	2	1	16	2	1	1.39200	48.401	4.0	
17	2	2	17	2	2	1.37300	49.891	1.0	
18	3	0	18	3	0	1.28840	54.702	8.0	
19	3	0	19	3	0	1.25980	56.684	2.0	
20	3	0	20	3	0	1.23080	58.823	1.0	
21	3	1	21	3	1	1.22880	58.833	1.0	
22	3	1	22	3	1	1.19980	60.293	2.0	
23	3	2	23	3	2	1.19750	60.345	1.0	
24	3	1	24	3	1	1.18420	60.844	2.0	
25	3	1	25	3	1	1.18360	60.852	3.0	
26	3	2	26	3	2	1.15320	63.069	1.0	
27	3	0	27	3	0	1.14330	63.204	1.0	
28	3	0	28	3	0	1.13430	63.322	1.0	
29	3	1	29	3	1	1.08150	65.065	2.0	
30	4	0	30	4	0	1.06330	66.088	1.0	
31	4	0	31	4	0	1.04760	67.034	1.0	
32	4	0	32	4	0	1.04350	67.243	1.0	
33	4	1	33	4	1	1.03470	67.799	2.0	
34	4	2	34	4	2	1.03300	67.828	1.0	
35	4	0	35	4	0	0.98950	69.609	1.0	
36	4	1	36	4	1	0.98730	69.633	1.0	
37	4	0	37	4	0	0.97830	70.473	1.0	
38	4	2	38	4	2	0.97620	70.528	1.0	
39	4	2	39	4	2	0.96980	70.833	1.0	

Stack Pattern

2 of 3

Date: 5/1/2022 Time: 3:43:56 PM File: 8% wt User: BAA394L PDSH 2-1



BORANG PENGESAHAN STATUS LAPORAN PROJEK SARJANA

TAJUK: A PRELIMINARY STUDY OF POROUS CERAMICS WITH LOW THERMAL CONDUCTIVITY FOR APPLICATION IN BUILDINGS

SESI PENGAJIAN: 2020/21 Semester 1

Saya **NAJMI ABDUL FATTAH BIN MOHD SALLEH**

mengaku membenarkan tesis ini disimpan di Perpustakaan Universiti Teknikal Malaysia Melaka (UTeM) dengan syarat-syarat kegunaan seperti berikut:

1. Tesis adalah hak milik Universiti Teknikal Malaysia Melaka dan penulis.
2. Perpustakaan Universiti Teknikal Malaysia Melaka dibenarkan membuat salinan untuk tujuan pengajian sahaja dengan izin penulis.
3. Perpustakaan dibenarkan membuat salinan tesis ini sebagai bahan pertukaran antara institusi pengajian tinggi.
4. ****Sila tandakan (✓)**

☐

SULIT

(Mengandungi maklumat yang berdarjah keselamatan atau kepentingan Malaysia sebagaimana yang termaktub dalam AKTA RAHSIA RASMI 1972)

☐

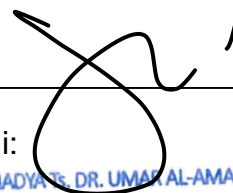
TERHAD

(Mengandungi maklumat TERHAD yang telah ditentukan oleh organisasi/badan di mana penyelidikan dijalankan)

☒

TIDAK TERHAD

Disahkan oleh:



Cop Rasmi:

PROFESOR MADYATIS, DR. UMAM AL-AMANI BIN HJ AZLAN
Dekan
Fakulti Teknologi Kejuruteraan Mekanikal Dan Pembuatan
Universiti Teknikal Malaysia Melaka

Alamat Tetap:

No 102 Jalan Padi Malinja 2

Bandar Baru UDA, 81200

Johor Bahru, Johor

Tarikh: 18/1/2022

Tarikh: 18/1/2022

**** Jika tesis ini SULIT atau TERHAD, sila lampirkan surat daripada pihak berkuasa/organisasi berkenaan dengan menyatakan sekali sebab dan tempoh laporan PSM ini perlu dikelaskan sebagai SULIT atau TERHAD.**